SYNTHESIS OF SOME METALOPHTHALOCYANINES AND THEIR EFFECTS ON THE PERFORMANCE OF PEM FUEL CELLS

A THESIS SUBMITTED TO
THE GRADUATE SCHOOL OF NATURAL AND APPLIED SCIENCES
OF
MIDDLE EAST TECHNICAL UNIVERSITY

BY

SERDAR ERKAN

IN PARTIAL FULFILLMENT OF THE REQUIREMENTS
FOR
THE DEGREE OF MASTER OF SCIENCE
IN
CHEMICAL ENGINEERING

SEPTEMBER 2005

Approval of the Graduate School of Natural and Applied Sciences

_____

Prof. Dr. Canan ÖZGEN
Director

I certify that this thesis satisfies all the requirements as a thesis for the degree of Master of Science.

_____

Prof. Dr. Nurcan BAÇ
Head of Department

This is to certify that I have read this thesis and that in my opinion it is fully adequate, in scope and quality, as a thesis for the degree of Master of Science.

_____	_____
Prof. Dr. Lemi TÜRKER	Prof. Dr. İnci EROĞLU
Co-Supervisor	Supervisor

Examining Committee Members

Prof. Dr. Işık Önal	(METU, CHE)	_____
Prof. Dr. İnci Eroğlu	(METU, CHE)	_____
Prof. Dr. Lemi Türker	(METU, CHEM)	_____
Prof. Dr. Saim Özkar	(METU, CHEM)	_____
Dr. Alper Tapan	(Gazi Univ., CHE)	_____

I hereby declare that all information in this document has been obtained and presented in accordance with academic rules and ethical conduct. I also declare that, as required by these rules and conduct, I have fully cited and referenced all material and results that are not original to this work.

Name, Last name : Serdar ERKAN

Signature :

ABSTRACT

SYNTHESIS OF SOME METALOPHTHALOCYANINES
AND
THEIR EFFECTS ON THE PERFORMANCE OF PEM FUEL CELLS

Erkan, Serdar
M.S., Department of Chemical Engineering
Supervisor : Prof. Dr. İnci Eroğlu
Co-Supervisor: Prof. Dr. Lemi Türker

September 2005, 97 pages

Importance of clean, sustainable and renewable energy sources are increasing gradually because of either being environmental friendly or being alternative for fossil fuels. Hydrogen energy system will let the utilization of alternative energy sources. Fuel cells are the most suitable energy conversion devices while passing through the hydrogen economy. The cost of the fuel cell systems need to be reduced in order to achieve commercialization of these systems. One of the most important cost items is platinum which is used as catalyst both in anode and cathode sides of the proton exchange membrane (PEM) fuel cells. Not only is the cost of the platinum, but also the limited reservoir of the platinum is a handicap. Therefore, the utilization of the cheap replacements of platinum catalysts will accelerate the process of commercialization. Because of their highly conjugated structure and high chemical stability metalo phthalocyanines have been encouraging electrocatalytic activity for oxygen reduction. Therefore, electrocatalytic activity for oxygen reduction in fuel cells was studied with some metalo phthalocyanines and some positive effects have been observed.

In this study, phthalocyanines of cobalt, iron and nickel were synthesized via phthalic anhydride-urea method and characterized by IR Spectrophotometry, X-Ray Diffractometry and Thermal Gravimetry (TGA). Catalyst materials were prepared by impregnation method such that they contain either 4% cobalt, 4% or 10% iron or 4% nickel phthalocyanines on carbon black (Vulcan XC72) structure. Impregnated catalysts were pyrolyzed at 600^{o}C or 1000^{o}C and cathode electrodes were prepared by these catalysts as well as unpyrolyzed ones by spraying technique. The impregnated catalysts were characterized by scanning electron microscopy (SEM) and pore structures were analyzed by surface area analyzer (by BET and BJH techniques). All of the anode electrodes were prepared by using 20% Pt containing commercial catalyst by the same technique applied for cathode electrodes. A membrane electrode assembly was also prepared by 20% Pt containing commercial catalyst on the cathode electrode. Performance characteristics of the manufactured membrane electrode assemblies were determined by means of a test station, built in Middle East Technical University Chemical Engineering Department, having a 5 cm^2 test cell.

The highest performance observed with the commercial membrane electrode assembly was 0.40W/cm^2 at 0.5 V. Whereas, the power density obtained from the MEA manufactured at the laboratory having 0.4 mg Pt/cm^2 loading both on the anode and cathode was 0.18 W/cm^2 at 0.5 V. For the phthalocyanine cathodic MEAs, the highest power reached was 0.04W/cm^2 which was obtained from the MEA having a loading of 0.28mg Co/cm^2 prepared by using the CoPc/C catalyst pyrolyzed at 1000 ^{o}C.

Keywords: Fuel cell, cobalt phthalocyanine, iron phthalocyanine, nickel phthalocyanine cathode catalyst, proton exchange membrane.

ÖZ

BAZI METALOFİTALOSİYANİNLERİN SENTEZİ VE
YAKIT HÜCRESİ PERFORMANSI ÜZERİNDEKİ ETKİLERİNİN
ARAŞTIRILMASI

Erkan, Serdar
Y. L., Kimya Mühendisliği Bölümü
Tez Yöneticisi : Prof. Dr. İnci Eroğlu
Ortak Tez Yöneticisi: Prof. Dr. Lemi Türker

Eylül 2005, 97 sayfa

Temiz, sürdürülebilir ve yenilenebilir enerji kaynaklarının önemi, ya çevre dostu olmaları ya da fosil yakıtlara seçenek olmaları nedeniyle giderek artmaktadır. Hidrojen enerji sistemi ise bu alternatif enerji kaynaklarının kullanılmasına olanak sağlayacaktır. Yakıt pilleri, hidrojen ekonomisine geçerken en uygun enerji dönüşüm aracı olarak görünmektedir. Yakıt pili sistemlerinin ticarileşmesinin sağlanabilmesi için sistem maliyetinin azaltılması gerekmektedir. Proton değişim zarlı yakıt pillerinin hem anot hem de katot tarafında katalizör olarak kullanılan platin en önemli maliyet kalemlerinden biridir. Platinin sadece maliyetinin değil, ayrıca rezervinin de kısıtlı olması da engel teşkil etmektedir. Dolayısıyla, platin katalizörlerin ucuz muadillerinin kullanımı ticarileşme sürecini hızlandıracaktır. Metalo fitalosiyaninler, yüksek derecede konjuge yapıları ve yüksek kimyasal kararlılıkları nedeniyle oksijen indirgenmesi için ümit verici elektro-katalitik aktiviteye sahiptirler. Dolayısıyla, bazı metalo

fitalosiyaninler yakıt pillerinde oksijen indirgenmesi için çalışılmış ve olumlu etkiler gözlenmiştir.

Bu çalışmada, kobalt, demir ve nikel fitalosiyaninler fitalik anhidrit-üre yöntemiyle sentezlenmiştir ve infrared spektrometri, x-ışını kırınımı ve ısıl gravimeri analizleri ile tanımlanmıştır. Katalizörler ya %4 kobalt, %4 veya %10 demir ya da %4 nikel fitalosiyaninlerin karbon siyahına (Vulcan XC-72) emdirilmesi yöntemiyle hazırlanmıştır. Emdirme işlemi yapılmış katalizörlere 600^{o}C veya 1000^{o}C de ısıl bozunma işlemi yapılmış ve bu katalizörlerle ve ayrıca ısıl bozunma işlemi yapılmamış katalizörlerle püskürtme tekniği kullanılarak katot elektrotları hazırlanmıştır. Fitalosiyanin emdirilmiş katalizörler taramalı elektron mikroskopisi (SEM) ve por yapıları yüzey alanı analiz cihazı (BET ve BJH teknikleri) ile tanımlanmıştır. Bütün anot elektrotları %20 platin içeren ticari katalizör kullanılarak, katot elektrotlara uygulanan yöntem kullanılarak hazırlanmıştır. Bu çalışmada hazırlanan metal fitalosiyanin içeren katalizörlerin performanslarının platin katalizörle karşılaştırılması için, bir zar elektrot yapısının katot elektrotu, %20 platin içeren ticari katalizörle hazırlanmıştır. Ayrıca, hazırlanan bütün zar elektrot yapılarının performansları ticari bir zar elektrot yapısı ile karşılaştırılmıştır. Üretilen zar elektrot yapılarının performans özellikleri, 5cm^{2}'lik bir test pili ile Orta Doğu Teknik Üniversitesi Kimya Mühendisliği Bölümü'nde kurulan yakıt pili test istasyonunda belirlenmiştir.

Ticari zar elektrot yapısı ile elde edilen en yüksek güç yoğunluğu 0.5 Volt ta 0.40W/cm^{2} olarak elde edilmiştir. Laboratuarda hazırlanan anot ve katotta 0.4 mg Pt/cm^{2} yüke sahip zar elektrot yapısının güç yoğunluğu ise 0.5 Volt ta 0.18 W/cm^{2} olarak elde edilmiştir. Fitalosiyanin katotlu zar elektrot yapıları için en yüksek ulaşılan güç 0.04 W/cm^{2} olup, bu değere, 1000^{o}C'de piroliz edilen CoPc/C katalizör kullanılarak hazırlanan 0.28mg Co/cm^{2} yüke sahip zar elektrot yapısı ile ulaşılmıştır.

Anahtar Kelimeler: Yakıt pili, kobalt fitalosiyanin, demir fitalosiyanin, nikel fitalosiyanin, katot katalizörü, proton değişim zarı.

To My Family

ACKNOWLEDGMENTS

I would like to express my deepest gratitude to my thesis supervisor, Prof. Dr İnci Eroğlu for her invaluable guidance, encouragement, humanity and insight throughout the research.

I would also like to express my gratitude to my thesis co-supervisor Prof. Dr. Lemi Türker for his creative suggestions, comments and guidance.

I am grateful to Prof. Dr. Nurcan Baç for his fuel cell hardware support which enabled me to get hints of a fuel cell to save invaluable time.

My special thanks go to my lab mate Ayşe Bayrakçeken, without her explanations and experience on the subject, I could not develop all of the abilities, methods and the technology by myself in a short time. Also, the brainstorming we made resulted the better understanding of the fuel cell concept.

I would like to thank Deniz Gürhan, my great friend, for his role in getting contact with Prof. Dr. İnci Eroğlu for this study. Not only on this occasion, but he always helpes me when I need help. I would like to express my gratitude to my friends, Gaye Çakal, Anıl Erdoğdu, Ela Eroğlu, Hakan Önder Olcay and Mustafa Öztürk for their valuable advices, helps and encouragements.

I wish to thank my friends Berker Fıçıcılar and Canan Şener for their help and suggestions about the characterization work of my thesis.

I would also like to thank Selçuk and Ayşegül Gümüş for their valuable help in the synthesis of metalo phthalocyanines. Finally, I would like to thank Ms. Kerime Güney,

Mrs. Gülten Orakçı, for their help in the chemical and physical analyses. Besides I would like to thank all the members of the workshop for their help.

This study was supported by TUBITAK with Project MISAG 230, METU BAP2004-07-02-00-128 and the State Planning Organization (DPT) Grant No: BAP-08-11-DPT2002K120510 (ÖYP-FBE-BTEK3).

TABLE OF CONTENTS

LIST OF TABLES

TABLES

LIST OF FIGURES

FIGURES

LIST OF SYMBOLS

A	slope of the Tafel line
E (V)	reversible (EMF) OCV
E^0 (V)	reversible (EMF) OCV standard pressure
F	Faraday constant, 96485 coulombs
ΔG_f (J/mol)	change in Gibbs free energy of formation
i (mA)	current density
i_n (mA)	internal and fuel crossover equivalent current density
i_0 (mA)	exchange current density
m , n	constants in the mass transfer overvoltage
P_x bar	partial pressure of the gas x
R	gas constant
r ohm/cm	area specific resistance
T (K)	temperature in K
V	voltage of the cell
ΔV_{act} (V)	voltage drop due to activation over voltage losses
ΔV_{ohm} (V)	voltage drop due to ohmic losses
ΔV_{trans} (V)	voltage drop due to mass transport losses
W_{elec} (J)	work done by the electrical cell
$W^{\max}$ (J)	maximum work

CHAPTER 1

INTRODUCTION

Energy is the most important requirement of modern human being. The consequence of technological development achieved is more intense energy requirement to sustain the comfort level reached. Energy is required for industry, transportation, communication, entertainment, interior air conditioning, etc. That is, energy consumption is inevitable in the modern world. Either due to lack of the conventional fuels or the environmental issues, alternative energy resources are required for the sustainable future. For the last few decades, hydrogen has been accepted as the most promising energy system and the researches have been focused on the production, storage and utilization of hydrogen for the generation of useful energy from primary energy sources. Hydrogen is a secondary form of energy that is reliable, easily transportable and convertible to other forms of the energy. Electricity is generated by the effective utilization of the hydrogen with oxygen in fuel cells have been researched and developed in the last few decades.

Fuel cells are electricity generators which are converting chemical energy of hydrogen directly to electricity by means of electrochemical oxidation and reduction reactions. While the operation of them is similar to batteries without any mechanical parts, the electricity generation is continuous as the case in mechanical electricity generators.

In a typical fuel cell, gaseous fuels are fed continuously to the anode compartment (negative electrode) and an oxidant (i.e., oxygen from air) is fed continuously to the cathode compartment (positive electrode); the electrochemical reactions take place at the electrodes to produce an electric current(Fuel Cell Handbook, 2000).

Because of the direct energy conversion fuel cells work at a higher efficiency than any other energy conversion process which involves a conventional heating cycle. The latter types are limited by the Carnot's cycle. Figure 1.1 shows a comparison of the conversion routes of fossil fuels to electricity in a fuel cell and in a conventional system such as a heat engine. One obvious aspect is that fewer steps are involved in the fuel cell process than in the conventional process. In addition, the conventional process exhibits lower conversion efficiency due to thermodynamic limitations. In a conventional process the chemical energy of fossil fuels is converted to electrical energy after several steps comprising a chemical reactor, mechanical engines and electrical generators, each step causes energy losses; thus, a fuel cell can directly convert chemical energy in electrical energy, minimizing the losses (Ullmann, 2002).

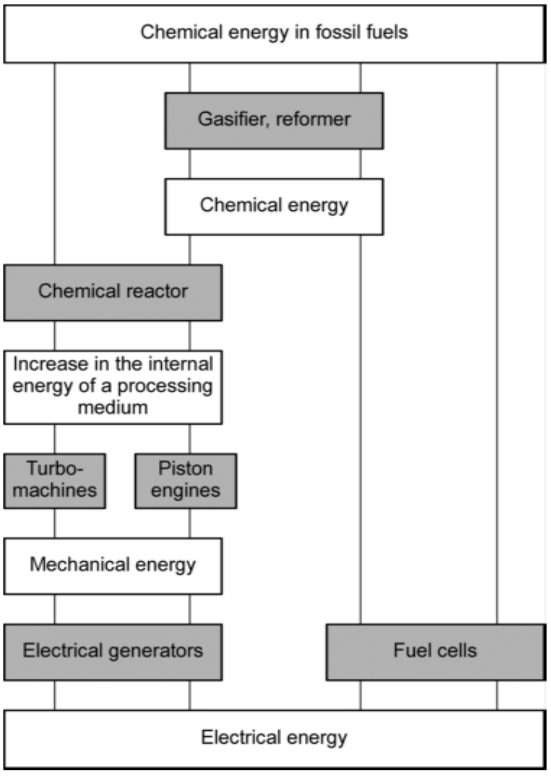

Figure 1.1 Comparison between the two conversion routes of fossil fuel into electric energy (Ullmann, 2002).

Fuel cells are quiet and operate with virtually no noxious emissions, but they are sensitive to certain fuel contaminants, e.g., CO, H_2S, NH_3, and halides, depending on the type of fuel cell. These contaminants must be minimized in the fuel gas. The two primary impediments to the widespread use of fuel cells are high initial cost and short operational lifetime. These two aspects are the focus of research (Kirk Othmer, 1992).

1.1. Types of the Fuel Cells

There is no perfect type of fuel cell. The electrolyte and the operating temperature of the fuel cell differ according to the fuel used. A fundamental technical problem of the fuel cells is stated as the slow reaction rates, leading to low currents and power (Larminie and Dicks, 2003). Therefore, many different fuel cell types are investigated. According to the type of electrolyte used in the cells, fuel cells are usually classified as polymer electrolyte fuel cell (PEFC) or polymer exchange membrane fuel cell (PEMFC), alkaline fuel cell (AFC), phosphoric acid fuel cell (PAFC), molten carbonate fuel cell (MCFC), and solid oxide fuel cell (SOFC) (Kirk Othmer, 1992).

1.1.1. Proton Exchange Membrane Fuel Cells (PEMFC)

As the name implies, a solid polymeric membrane is used as an electrolyte in this type of fuel cells. Compact and high energy density fuel cells can be achieved in this type. This solid membrane allows wide power ranges of fuel cells to be built.

The first prototype of PEMFC was produced by General Electric (GE) in 1963. A 1 kW system was realized for the Gemini mission of NASA with a sulfonated polystyrene membrane as electrolyte, the cell was operated with pure gases. In 1969 Nafion® (Du Pont) was used as electrolyte in a GE fuel cell for the first time. In the 1980s Ballard

Power System began with a project on PEMFC and also used a proton exchange membrane produced by DOW Chemical. A five-cell-stack using air as oxidant was presented in 1988; similar systems of varying power were used by Ballard (Ullmann, 2002).

As introduced by Kirk Othmer (1992), the advantages of PEMFCs are

- no free corrosive liquid in the cell,
- simple fabrication of the cell,
- ability to withstand large pressure differentials,
- materials corrosion problems are minimal, and
- demonstrated long life.

On the other hand, the disadvantages of PEMFCs are that

- the fluorinated polymer electrolyte is traditionally expensive,
- water management in the membrane is critical for efficient operation, and
- long-term high performance with low catalyst loadings in the electrodes needs to be demonstrated.

The reactions involved in the PEM fuel cells are given in Equations 1 and 2.

at the anode; $2H_2 \rightarrow 4H^+ + 4e^-$ $E^o = 0$ V (1)

at the cathode $4H^+ + O_2 + 4e^- \rightarrow 2H_2O$ $E^o = 1.229$ V (2)

Then, the standard potential of the cell becomes $E^o_{cell} = 1.229$ V.

1.1.2. Alkaline Fuel Cells (AFC)

Alkaline fuel cells are low operating temperature fuel cells. Instead of solid polymeric membrane, an alkaline material, usually potassium hydroxide is used as electrolyte.

The first alkaline fuel cell was build by BACON in the mid 1950s, it was a 5 kW system with 30 % aqueous KOH as the electrolyte, operating at 200 °C and 5 MPa, reactants were pure gases. NASA used slightly modified Bacon cells for the Apollo program, the technical features of the Apollo fuel cells were: 85 % KOH as the electrolyte, 230 °C operating temperature, 0.33 MPa pressure, pure gases as reagents, stack power 1.5 kW, and up to 11 000 h operation at the mission end. NASA improved the AFCs for the space shuttle program. The stack power was increased to 12 kW, and the operating temperature lowered to 90 °C. They operated with pure gases and a specific power of 275 W/kg. Nickel plates were used as interconnectors, Pt–Pd mixtures were employed as anodic, whereas, Au–Pt mixtures as cathodic catalysts. Lifetimes up to 15 000 h were observed (Ullmann, 2002).

The reactions take places in AFC are given in Equations 3 and 4.

at the anode $H_2 + 2\,OH^- \rightarrow 2\,H_2O + 2\,e^-$ (3)

at the cathode $1/2\,O_2 + 2\,e^- + H_2O \rightarrow 2\,OH^-$ (4)

1.1.3. Phosphoric Acid Fuel Cell (PAFC)

Phosphoric acid concentrated to 100% is used for the electrolyte in these types of fuel cells, which operates at 150 to 220^{o}C. At lower temperatures, phosphoric acid is a poor ionic conductor, and CO poisoning of the Pt electrocatalyst in the anode becomes severe. The relative stability of concentrated phosphoric acid is high compared to other common acids; consequently a PAFC is capable of operating at the high end of the acid temperature range (100 to 220^{o}C). In addition, the use of concentrated acid (100%) minimizes the water vapor pressure so water management in the cell is not difficult. The matrix universally used to retain the acid is silicon carbide, and the electrocatalyst in both the anode and cathode is Pt (Fuel Cell Handbook, 2000). The reactions are the same as in the PEM fuel cells given in Equations 1 and 2.

1.1.4. Molten Carbonate Fuel Cell (MCFC)

The electrolyte in these fuel cells is usually a combination of alkali carbonates, which is retained in a ceramic matrix of $LiAlO_2$ or MgO. The fuel cell operates at 600 to 700^oC so that the alkali carbonates form a highly conductive molten salt, with carbonate ions providing ionic conduction. At the high operating temperatures in MCFCs, Ni (anode) and nickel oxide (cathode) are adequate to promote reaction. Noble metals are not required (Fuel Cell Handbook, 2000).

The operating principles of a MCFC comprise the reactions given in Figure 5 and 6.

Anode: $$H_2 + CO_3^{2-} \rightarrow H_2O + CO_2 + 2e^- \quad (5)$$

Cathode: $$1/2\,O_2 + CO_2 + 2e^- \rightarrow CO_3^{2-} \quad (6)$$

The mobile ions are CO_3^{2-} ions which move from the cathode to the anode through the molten Li, K, and Na carbonates immobilized in $LiAlO_2$ or MgO matrix, the water is produced at the anode. Water is removed together with CO_2, possible traces of CO react at the anode with H_2O, forming CO_2 and H_2. Therefore, it is very convenient to use MCFC with fuels such as natural gas or other hydrocarbons (Ullmann, 2002).

1.1.5. Solid Oxide Fuel Cell (SOFC)

The solid oxide fuel cell (SOFC) operates in the temperature range of 600 to 1000^oC. This means that high reaction rates can be achieved without expensive catalysts, and that gases such as natural gas can be used directly, or “internally reformed” within the fuel cell, without the need for a separate unit. This fuel cell type thus addresses all the problems and takes full advantage of the inherent simplicity of the fuel cell concept. Nevertheless, the ceramic materials that these cells are made from are difficult to handle,

so they are expensive to manufacture. Also, the auxiliary units such as air and fuel pre-heaters and cooling system are complex and not easy to start up (Larminie and Dicks, 2003).

1.1.6. Summary of Fuel Cell Types

The differences of the fuel cell types can be summarized as in Table 1.1. The major differences of the fuel cell types are based on the electrolyte used, the operating temperature, the charge carrier, the requirement of an external reformer, the prime cell components, the catalyst used, and water and heat management.

Table1.1 Summary of Major Differences of the Fuel Cell Types (Fuel Cell Handbook, 2000)

	PEMFC	**AFC**	**PAFC**	**MCFC**	**ITSOFC**
Electrolyte	Ion Exchange Membranes	Mobilized or Immobilized Potassium Hydroxide	Immobilized Liquid Phosphoric Acid	Immobilized Liquid Molten Carbonate	Ceramic
Operating Temperature	80°C	65°C - 220°C	205°C	650°	600-800°C
Charge Carrier	H^+	OH^-	H^+	$CO_3^=$	$O^=$
External Reformer for CH_4 (below)	Yes	Yes	Yes	No	No
Prime Cell Components	Carbon-based	Carbon-based	Graphite-based	Stainless-based	Ceramic
Catalyst	Platinum	Platinum	Platinum	Nickel	Perovskites*
Product Water Management	Evaporative	Evaporative	Evaporative	Gaseous Product	Gaseous Product
Product Heat Management	Process Gas Independent Cooling Medium	Process Gas Electrolyte Calculation	Process Gas Independent Cooling Medium	Internal Reforming Process Gas	Internal Reforming Process Gas

(*) Perovskites are large family of crystalline ceramics that derive their name from a specific mineral known as perovskite ($CaTiO_3$) due to their crystalline structure

1.2. The Components of the Proton Exchange Membrane (PEM) Fuel Cells Needed to be Improved

Proton exchange membrane fuel cells have various advantages among the other types of fuel cells. The ease of handling and relatively compact size due to solid polymer membrane makes PEM fuel cells applicable to low and medium power range applications. Moreover, the quick start-up and relatively fast response time are the other important features of PEM fuel cells for the applications, either mobile or stationary. Therefore, the researches have been focused on the PEM fuel cells in the near past. Even though the PEM fuel cell system seems to be a simple device, there are some problems for the commercialization of them. Three main components of the PEM fuel cells are ion exchange membrane, hardware material for gas distribution and current collection plates and catalyst for both anode and cathode.

As the name implies the main component is the ion exchange membrane. The well-known and widely used ion exchange membrane is Nafion®. The membrane is a significant cost item on the overall system cost. Not only the cost of the membrane is a problem, but also it has technical weaknesses such that it has to be kept on the fully hydrated condition which requires critical water management. It is known that the leading fuel cell company Ballard uses membranes produced by Dow Chemicals which requires lower hydration levels. Many researchers are focused on the membrane development in order to decrease the cost and increase the ion conductivity for lower hydration levels.

The other component needed to be developed is the hardware material for the gas distribution and current collection plates. Graphite is used in the today's limited number of prototype fuel cells. The reason of using graphite is that it is durable in the corrosive medium of the fuel cell in the long run. However, the cost of manufacture of machined

gas channel plates is high. In the previous years, these plates were started to be produced by injection molding which resulted to decrease the cost of these plates for the high volume production.

Another important component is the catalyst. A PEM fuel cell operates at low temperature range which is below 100 ^{o}C for today. In the next coming years, the operating temperature might be extended to 150^{o}C depending on the developments in the field of membrane. That is, the temperature range of the operation is not enough for achieving fast reaction kinetics without a high activity catalyst. Therefore, platinum is used in order to achieve high reaction rates both in the anode and cathode in the PEM fuel cells. Since platinum is an expensive noble metal, the amount of it used in the fuel cell system must be reduced. Not only is the cost of the platinum, but also the limited reservoir of the platinum is a handicap. Therefore, the utilization of cheap replacements of platinum catalysts will accelerate the process of commercialization.

Because of their highly conjugated structure and highly stable metalo phthalocyanines have an encouraging electrocatalytic activity for oxygen reduction. Therefore, electrocatalytic activity for oxygen reduction in fuel cells was studied with some metalo phthalocyanines and positive effects have been observed (Wang et.al., 1999). Further studies can reveal the catalytic potential of the phthalocyanines with different transition metals.

1.3. The Objective of the Study

Extensive research has been carried out on the renewable and alternative energy resources. The most promising of these alternative energy resources is hydrogen. Although the hydrogen is not a primary energy source, it can be easily produced by using the completely renewable and environmentally benign primary energy sources such as solar and wind energy and also the fossil fuels in the transition period to the hydrogen energy economy. It is believed that the hydrogen energy utilization will be

achieved by fuel cells. The highly efficient and the environmentally friendly operation of the fuel cells make them the energy converters of the future.

Some problems are required to be solved in order to achieve the commercialization of the fuel cells. The main handicap is the cost of the system which is mainly due to the catalyst material platinum. Therefore, the studies resulting in the utilization of non-noble metal catalysts would be very beneficial for the commercialization of the fuel cells.

The objective of present work is to prepare and develop some metalo phthalocyanine catalysts for oxygen reduction at the cathode side of a polymer electrolyte fuel cell and to test the performance of the PEMFC using the prepared catalyst and compare its performance with platinum containing commercial catalysts.

In order to achieve the first part of this task, the synthesis of cobalt, iron and nickel phthalocyanines were synthesized by phthalic anhydride-urea process. These metalo phthalocyanines were loaded into the carbon black support by impregnation method. The catalytic effect of these phthalocyanines was investigated by producing membrane electrode assemblies by a newly developed manufacturing technique and testing the fuel cells assembled with these membrane electrode assemblies.

CHAPTER 2

LITERATURE SURVEY

Literature survey is presented in six parts. The proton exchange membrane fuel cells are considered in the first part. Whereas, the second part concentrates on the potential of metalo phthalocyanines as cathode catalyst in a fuel cell. The syntheses of various metalo phthalocyanines are discussed in part three. In the fourth part, the preparation of suitable catalysts from metalo phthalocyanines and platinum for fuel cells is explained. In order to perform the performance tests of the prepared catalysts, membrane electrode assemblies are required to be prepared. Hence, part five explains the methods of preparation of membrane electrode assemblies. Finally, the evaluation of the performances in a test cell is explained in part six.

2.1. Proton Exchange Membrane (PEM) Fuel Cells

Proton exchange membrane fuel cells (PEMFC) deliver high power density, which offers low weight, size and cost. The immobilized electrolyte membrane simplifies sealing in the production process, reduces corrosion, and provides for longer cell and stack life. PEMFCs operate at low temperature, allowing for faster startups and immediate response to changes in the demand for power. The PEMFC system is seen as the system of choice for vehicular power applications, but is also being developed for smaller scale stationary power (Fuel Cell Handbook, 2000).

2.1.1. The Mechanism of Polymer Ion-Exchange Membrane

The different companies producing polymer electrolyte membranes have their own special tricks, mostly proprietary. However, a common theme is the use of sulphonated fluoro-polymers, usually fluoroethylene. The most well known and well established of these is Nafion (®Dupont), which has been developed through several variants since the 1960s. This material is still the electrolyte against which others are judged, and is in a sense an 'industry standard'. Other polymer electrolytes function in a similar way (Larminie and Dicks, 2003).

In order to prepare a proton conducting polymer, the basic PTFE (teflon) polymer is "sulphonated" - a side chain is added, ending with sulphonic acid (HSO_3) group. The details of the sulphonation vary for different types of Nafion, and with different manufacturers of these membranes. The methods of creating and adding the side chains are proprietary, though one modern method is discussed in Kiefer et al. (1999) (Larminie and Dicks, 2003).

The hydrophilic regions around the clusters of sulphonated side chains can lead to the absorption of large quantities of water, increasing the dry weight of the material by up to 50%. Within these hydrated regions, the H^+ ions are relatively weakly attracted to the SO_3^- group and are able to move. This creates what is essentially a dilute acid. The resulting material has different phases - dilute acid regions within a tough and strong hydrophobic structure (Larminie and Dicks, 2003).

2.1.2. Catalysts Used for PEM Fuel Cells

The heart of the proton exchange membrane fuel cell (PEMFC) is the membrane electrode assembly (MEA) which consists of two catalyst layers at the two sides of the proton conducting membrane. These two catalyst layers play a critical role on the performance of the MEA. Without catalysts, the generation of energy is not possible (Hoogers, 2002).

As with any heterogeneous catalyst material, a number of fundamental requirements are necessary for good performance. These include high intrinsic activity of sites for the reaction and a maximum number of these sites. Additional requirements for fuel cells are (Hoogers, 2002):

- Electrical Conductivity
- Good interaction with ionomer
- Reactant gas access
- Stability in contact with reactants, products, and electrolytes

Research over several decades has found that platinum and platinum-containing catalysts are the most effective catalyst materials, in terms of both activity and stability. Recent efforts have been focused on learning how to use platinum more effectively. In general, to achieve the maximum number of active sites of a given active phase, dispersion of that phase on an inert support is required. In the case of low-temperature fuel cells, the support also needs to have the properties listed above. Conductive carbon black supports generally meet these requirements (Hoogers, 2002).

As carbon support, Vulcan XC-72 carbon black is the most widely used catalyst support both in the research studies and commercial applications. A small number of studies have been published on the effect of different carbon supports on catalyst properties. As cited in Hoogers (2002), Tokumitsu et al. (1999) reported that increasing the carbon surface from $60 m^2/g$ to over $1300 m^2/g$ leads to reduction in Pt particle size from 2.5 to 1.5 nm for 10 wt% catalysts. Similarly, Uchida et al. (1996) showed that Pt crystallite size decreased from 3.7 to 1.0 nm when the carbon surface area increased from 58 to 1500 m^2/g for a series of 23 to 24 wt% Pt catalysts. However, despite the increases in Pt surface area achieved by higher-area carbon supports, both these studies showed little effect of carbon support on activity. It was suggested that both the Pt particle size effect and the interaction of the ionomer with the carbon support played important roles in determining activity.

Yazaydın et al. (2003) investigated the effect of the carbon used on the performance of alkaline fuel cells. The study revealed the fact that the type of the carbon support material affects the overall performance of the alkaline fuel cells. The alkaline fuel cells manufactured with activated carbon used in electrode layer exhibited better performance than carbon black.

Although pure hydrogen can be fed to the anode, the stream may include CO and CO_2 also because of the economical reasons production method conducted. Also on site generation of hydrogen, namely, reformation of hydrocarbons would contain a significant amount of CO and CO_2. It is well known that CO binds to platinum irreversibly which results to deactivation of the catalyst due to the loss of the active sites. Although the effect of CO_2 is not significant as CO, the reverse water-gas shift reaction produces CO from CO_2.

The most elegant way to overcome anode poisoning is through the development of CO- and CO_2-tolerant electrocatalysts, which are capable of operating in the presence of at least 100 ppm CO and 20-25% CO_2, (Cooper et al., 1997).

The cathode reaction differs from that at the anode, as the cathode catalyst does not need to perform selective catalysis in most PEMFC applications except direct methanol fuel cells (DMFC). Pt based catalysts can catalyze both oxygen reduction and methanol (MeOH) oxidation, leading to mixed potentials. In acid electrolytes, noble metals such as Pt, Pd, and Rh and their alloys have been found to be the catalysts of choice for oxygen reduction. However, even the best of these catalysts, Pt, is at least 10^6 times less active for oxygen reduction than for H_2 reduction. This leads to high over potentials and is the major catalytic limitation to fuel cell efficiency (Hoogers, 2002).

Recent literature has shown that Ru-based chalcogenides, pyrolyzed Fe and Co macrocycles, and metal carbides all show significant oxygen reduction. In addition, many of these catalysts show good selectivity towards oxygen in the presence of methanol, which may allow some advantages when they are used as cathode catalysts in DMFCs (Hoogers, 2002).

2.2. Fuel Cell Performance

For an electrochemical cell the maximum work that can be obtained is equal to the change in Gibbs free energy of the process at constant temperature and pressure. That is,

$$W^{\max} = \Delta G_f \tag{7}$$

The maximum work is obtained if the process is sufficiently slow that there are no irreversibilities. The electrical potential produced by the cell is referred as zero-current cell potential (E). The work done by the electrical cell W_{elec}, in moving n moles of electrons across a potential difference of E is given in Equation 8.

$$W_{elec} = -nFE \tag{8}$$

Since $\Delta G_f = W_{elec} = -nFE$ (9)

and n=2 for a hydrogen fuel cell. Then the fundamental equation which gives the reversible zero-current voltage or reversible open circuit voltage E becomes,

$$E = \frac{-\Delta G_f}{2F} \tag{10}$$

where F is the Faraday constant and equal to 96485C. The values of the ΔG_f for the reaction H_2+1/2O_2 → H_2O at various temperatures are given in Table 2.1.

Table 2.1 ΔG_f for the reaction $H_2+1/2O_2 \rightarrow H_2O$ at various temperatures (Larminie and Dicks, 2003)

Form of water product	Temperature (^oC)	ΔG_f (kJ mol^{-1})
Liquid	25	-237.2
Liquid	80	-228.2
Gas	80	-226.1
Gas	100	-225.2
Gas	200	-220.4
Gas	400	-210.3
Gas	600	-199.6
Gas	800	-188.6
Gas	1000	-177.4

From the values of ΔG_f listed in Table 2.1, the ideal potential of a H_2/O_2 fuel cell as a function of temperature can be plotted as in Figure 2.1.

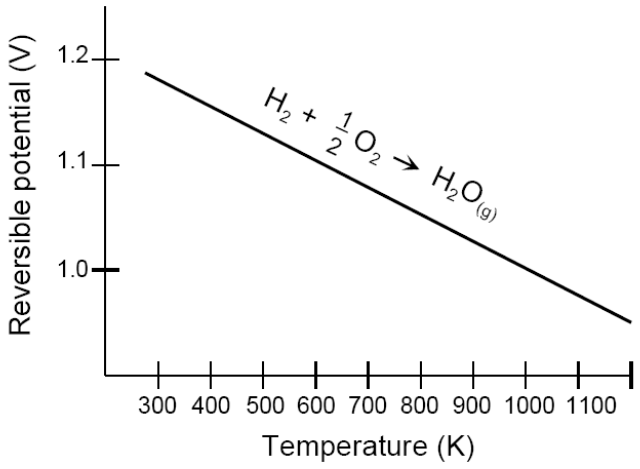

Figure 2.1 H_2/O_2 Fuel Cell Ideal Potential as a Function of Temperature (Fuel Cell Handbook, 2000)

The pressure and concentration of the reactants affect the Gibbs free energy, and thus the voltage. This situation can be described by Nernst equation given in Equation 11.

$$E = E^0 + \frac{RT}{2F} \ln\left(\frac{P_{H_2} \cdot P_{O_2}^{\frac{1}{2}}}{P_{H_2O}} \right) \tag{11}$$

where E^0 is the cell EMF at standard pressure.

For the actual operation of a fuel cell, even at the open circuit (zero-current) conditions, no loss (ideal) voltage of the cell could not be reached. The total loss of the cell voltage is composed of activation polarization loss, ohmic polarization loss, and the concentration polarization loss. A typical polarization curve containing the listed losses is given in Figure 2.2.

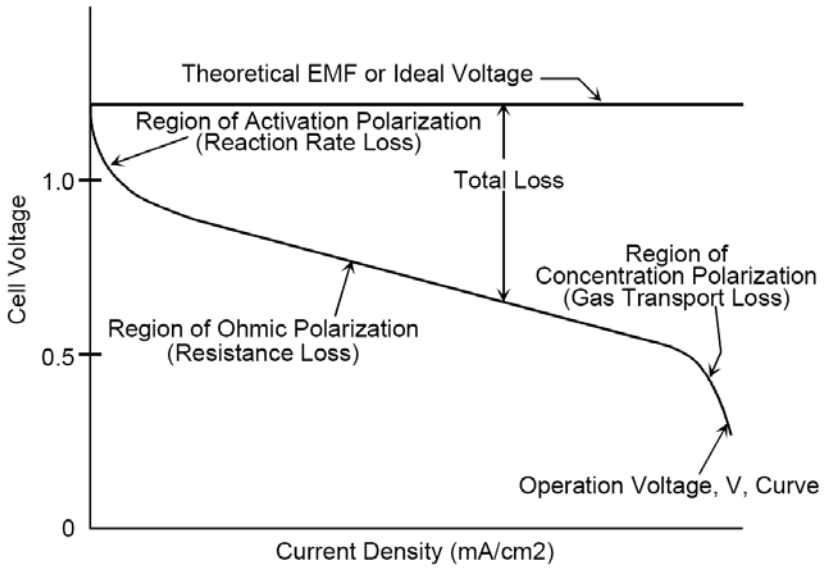

Figure 2.2 Ideal and Actual Fuel Cell Voltage/Current Characteristic (Fuel Cell Handbook, 2000)

The overall irreversibilities resulting the voltage loss can be described as in Equation 12

$$V = E - \Delta V_{ohm} - \Delta V_{act} - \Delta V_{trans} \tag{12}$$

substituting ohmic, activation and transport voltage losses into Equation 12 one gets Equation 13.

$$V = E - ir - A\ln\left(\frac{i + i_n}{i_0}\right) + m\exp(ni) \tag{13}$$

where, E is the reversible open circuit voltage (OCV), for a typical PEM fuel cell operating at room temperature E is about 1.2 V. Reversible OCV is a function of temperature which is given in Figure 2.1. i is the current density, that is, the current generated per unit active area of the fuel cell. The value of the current density is dependent on the electrical load applied at that instant. For the commercial fuel cells, the typical value of the current density is 1 A/cm^2 at 0.6 V operational voltage, currently. i_n is the internal and fuel crossover equivalent current density, i_0 is the Exchange current density at an electrode/electrolyte interface which has a typical value of 0.1 mA/cm^2 for a low temperature hydrogen-fed fuel cell running on air at ambient pressure for platinum catalyst. A is the slope of the Tafel line having a typical value of 0.06 V/decay , m and n are the constants in the mass transfer overvoltage. The value of m is typically about 3x10^{-5} V (Larminie and Dicks, 2003). Finally, r is the area specific resistance which has a value of less than 1ohm/cm^2 typically.

2.3. Catalytic Potential of Metalo Phthalocyanines

Base metal (e.g., Fe, Co) macrocyclic compounds (e.g., porphyrins, phthalocyanines, tetraazannulenes) have long been known to be able to electro-reduce dioxygen (Jahnke et al., 1979). Therefore, transition-metal organic macrocycles adsorbed on carbon have been studied for a number of years as potential electrocatalysts to replace Pt for oxygen

reduction (Wang et.al., 1999). In alkali, Co-based systems in particular show excellent performance and durability and are extensively used in metal-air battery systems (Gamburzev et al., 2001). However, in acid, although both Fe- and Co-based systems show oxygen reduction activity, both overall performance and durability are poor. Attempts to improve both these properties led to the discovery that heat-treating the catalysts at high temperature (600°C) did improve catalyst durability, but performance was still poorer than that of Pt-based systems (Gojkovic et al., 1999; Jiang and Chu, 2000) (as cited in Hoogers, 2002).

Lefevre et.al. (2000) stated that the best electrocatalytic activities had been shown to occur in the pyrolysis temperature range comprised between 500 and 700 °C. In that temperature range, the catalytic site is N_4-Metal bound to the carbon support. It was labeled the low temperature site. However, the use of these catalysts in a single membrane electrode assembly of a H_2/O_2 PEM fuel cell revealed that the low-temperature site was unstable and that pyrolysis temperatures $\geq$ 800 °C are necessary to obtain more stable catalysts.

Faubert et.al. (1998) studied different quantities of iron tetraphenylporphyrin (FeTPP) adsorbed onto carbon black (XC-72). Pyrolysis of the FeTPP was carried at 1000°C to produce catalysts containing iron loadings of 2, 4 and 6 wt%. The relative catalytic activities for oxygen reduction in polymer electrolyte fuel cells and in rotating disk electrode cells were obtained as 4 > 2 > 6 wt% Fe. All these catalysts demonstrated stable behavior in a fuel cell element at 0.5 V vs RHE and at 50°C until the 10th hour of operation when slow decaying of the catalytic activity began.

2.4. Synthesis of Metalo Phthalocyanines

As cited by Ullmann (2002), Linstead in 1933, described a class of organic dyes whose colors range from reddish blue to yellowish green as phthalocyanine. Phthalocyanine forms complexes with numerous metals of the periodic table.

Today, there are known 66 complexes with various elements. The most important metal phthalocyanines are derived from phthalodinitrile, phthalic anhydride, Phthalimide derivatives, or metal-free phthalocyanine by boiling the latter in quinoline with metal salt (Ullmann, 2002).

The chemical structures of cobalt, iron and nickel phthalocyanines are given in Figure 2.3. The only difference in the chemical structure of the different metal phthalocyanines is the central metal atom. However, the physical and chemical properties of the metal phthalocyanines slightly differ according to its central metal atom. The X-ray, physical and chemical data of the some metal phthalocyanines is listed in the Appendix part Figure C.1.

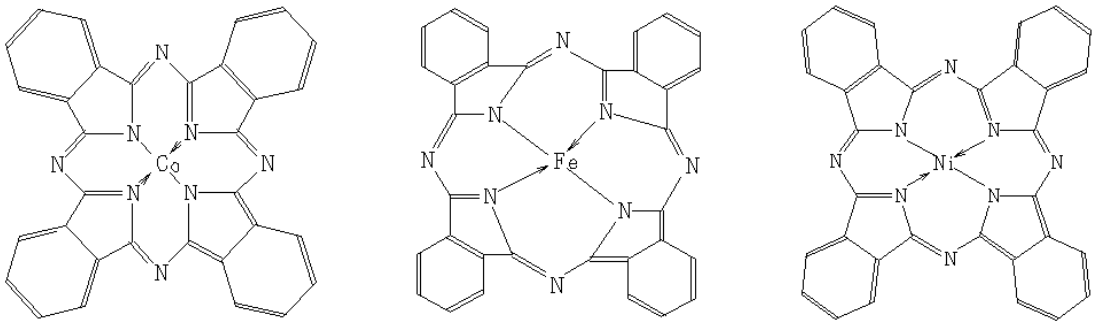

Figure 2.3 Chemical structures of the cobalt, iron and nickel phthalocyanines

Segawa et.al. (1990) improved the metal phthalocyanine production process called phthalic anhydride-urea process. In this process phthalic anhydride or its derivative is heated with urea and a metal salt or metal existence of a catalyst with a solvent. As the catalyst, a molybdenum compound such as ammonium molybdate, molybdic acid, phosphorus molybdic acid, and ammonium phosphorus molybdate or molybdenum oxide. Among them, ammonium molybdate is particularly superior. In addition to the

above, arsenic vanadium compound, boric acid or a halide or an oxyhalide of titanium, tin or antimony, may be used. As the solvent, thermally stable, inexpensive and inert to the reactants solvents can be used. In the industrial processes triclorobenzene or nitrobenzene are used.

Sakamoto and Ohno (1997) reported the synthesis of three kinds of cobalt phthalocyanine derivatives: cobalt phthalocyanine tetrasulfonic acids, cobalt phthalocyanine octacarboxylic acids and cobalt octakis (hexyloxymethyl) phthalocyanines, and a new type of phthalocyanine derivative, cobalt anthraquinocyanine.

Jung et.al. (2004) studied two different processes for the synthesis of copper phthalocyanines. The synthesis were carried out by reaction of phthalic anhydride, urea, and copper (I) chloride at various temperatures and times under classical and microwave processes. Scanning electron microscopy (SEM), X-ray diffraction (XRD), BET, and particle size analysis were performed for the characterization of the samples synthesized at various conditions. The best yield of 85.1 wt.% was obtained at 180 $^{\circ}$C for 4 h under the classical process and that of 88.2 wt.% was obtained at 170 $^{\circ}$C for 4 h under the microwave process. Comparison between the classical and microwave processes revealed that the non-thermal effects of microwaves were existed during reaction period because the reaction occurred at lower temperature in a very limited extension.

Oker (1985) was synthesized copper phthalocyanine by the well known method phthalic anhydride urea method and proposed the reaction steps of this synthesis method as given in Figure 2.4. The copper may either be supplied as copper bronze or as copper salts. In the study $CuCl_2$ and Cu_2C1_2 were selected as copper sources and their efficiency was compared by carrying out two sets of experiments. In the former the yield of the product (CuPC) was 10% smaller than that of the latter.

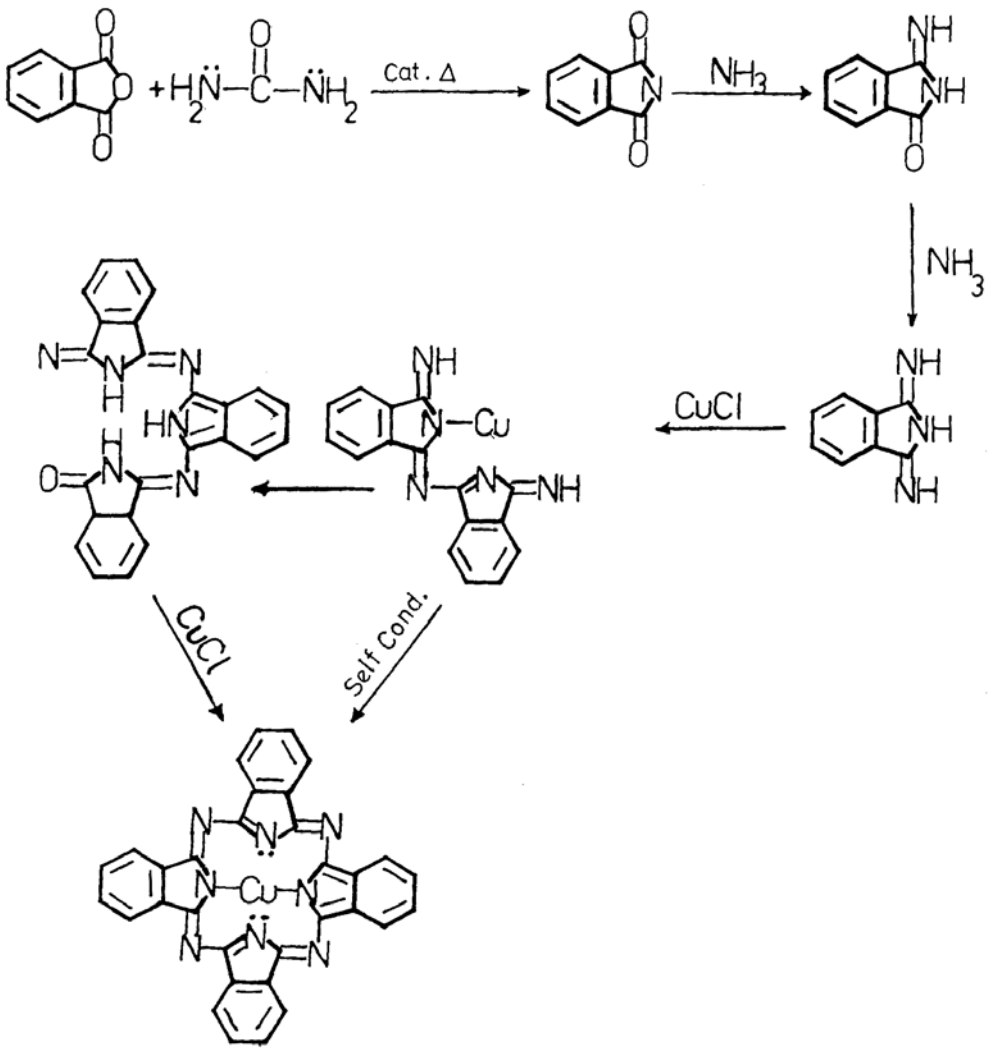

Figure 2.4 The reactions involved in Phthalic Anhydride-Urea Process (Oker, 1985)

Urea is the source of nitrogen and at the elevated temperatures urea decomposes and NH_3 is produced along with some urea decomposition products such as biureth which acts as halogen acceptors as formulated in the Figure 2.5.

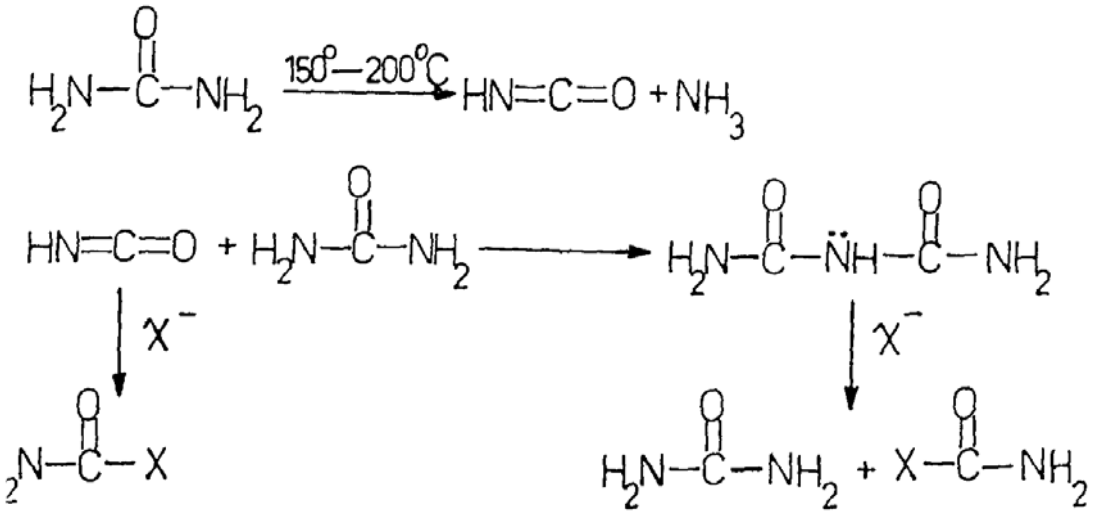

Figure 2.5 The reactions of the generation of NH_3 and removal of x^- (Oker, 1985)

2.5. Catalyst Preparation with Metalo Phthalocyanines

Van Veen and Visser (1979) prepared oxygen reduction catalysts with monomeric transition metal phthalocyanines. The supports were chosen as active carbon (Norit BRX) and high surface area graphite (henceforth HAS graphite). Both supports were gas and heat treated. Two methods were followed for the catalyst preparation. In the first method, the metal phthalocyanine (MePc) was dissolved in 96% H_2SO_4 and precipitated on the support by pouring into ice-water to yield MePc/support. The second method was conducted by contacting MePc and carbon with a solution of the former in pyridine with a continuous stirring of one day.

Tetracarboxylic cobalt phthalocyanine supported on carbon black (CoPcTc/C) was studied as an oxygen reduction catalyst by Lalande et.al. (1995). Carbon black (XC-72 from Cabot) was used as the supporting medium and CoPcTc was impregnated into the support. First, CoPcTc was dissolved in tetramethylammonium hydroxide $(CH_3)_4NOH$

at pH 13. In order to dissolve CoPcTc completely, overnight stirring was performed. Then XC-72 was added to the solution and stirred for 10 minutes. pH was reduced to about 2 by adding concentrated HCl. The tetracarboxylate in the solution precipitated as tetracarboxylic acid onto the carbon black. Then, the precipitate rinsed with methanol and water and dried. Resulting powder was heat-treated in Argon atmosphere at temperatures varying between 100 and 1100^{o}C.

Lalande et.al. (1996) studied the catalytic activity and stability of heat treated iron phthalocyanines. FePc and FePcTc were adsorbed onto carbon black (XC-72R from Cabot) containing 2 wt % iron. FePc or FePcTc were dispersed with XC-72R in anhydrous pyridine. The dispersion was stirred at reflux for 8 h under Ar. The slurry was then poured into 1 L of de-ionized water to precipitate the organic precursor onto the carbon black. For FePcTc, the precipitation was completed by lowering the pH to 2 with formic acid. The resulting material was then filtered, rinsed with de-ionized water and dried overnight at 75 °C in air. The catalysts were then heat-treated under Ar for 2 h at temperatures ranging from 100 to 1100 °C.

Kalvelage et.al. (2000) made experiments with iron and cobalt phthalocyanines and also cobalt and iron cyclames (CoCy, FeCy). Concentrated sulfuric acid was used as solvent for dissolving CoPc and FePc. Carbon black was added while the solution was constantly stirred. After one hour of stirring, the precipitation of the phthalocyanines on the carbon black was achieved by pouring the slurry into cold water. After another six hours of stirring, the slurry was filtered and washed in deionized water for several times. The pyrolysis of the catalyst-loaded carbon black samples was performed in the quartz tube of a tube oven. The heat treatment was performed under permanent nitrogen flow. The desired pyrolysis temperature was held for two hours.

2.6. Preparation of Membrane Electrode Assembly (MEA)

Membrane electrode assemblies (MEAs) are prepared in order to investigate the performances of the prepared catalytsts. There are many methods proposed for the preparation of MEAs.

Lalande et.al. (1996) performed fuel cells measurements for the metalo phthalocyanine catalysts with gas diffusion electrodes (GDE) in a fuel cell test station. The catalyst suspension for the cathode consisted of 17.1 mg of catalyst, 0.240 ml of de-ionized H_2O and 0.240 ml of 5 wt % Nafion recast solution blended ultrasonically for 1 h. The resulting thick paint was applied in 4 successive layers on a 1 cm^2 uncatalyzed electrode. Each layer consisted of 60 ml of the catalyst suspension. The paint was dried in air at 60 °C between the application of each layer and in a vacuum oven at 70 °C for 1 h after the deposition of the last coating. The iron metal loading in these cathodes was about 0.15 mg/cm^2. The anode consisted of a 1 cm^2 electrode catalyzed with 0.37 mg/cm^2 (20 wt %) Pt. Single cell assembly was prepared by pressing a Nafion 117 membrane between the anode and the cathode under 2500 psi at 140 °C for 40 s. Wang et.al. (1999) and Lefévre et.al. (2000) also applied similar technique.

The fabrication technique of the MEA was studied in detail by Song et.al. (2001). The complete fabrication of gas diffusion electrodes (GDE) was basically a three-step process; carbon paper first undergoes hydrophobic treatment, then a thin PTFE/carbon layer is cast onto the treated surface, and lastly the catalyst layer was cast onto the surface of the supporting layer. The catalyst layer was cast onto the PTFE/C layer surface from the catalyst suspension that was prepared by dissolving 20 wt % Pt/C and 5 wt % Nafion® solution in 2-propanol solvent. The Pt loading in the catalyst layer was fixed at 0.4 mg/cm^2 and the optimum Nafion concentration in the catalyst layer was found to be 0.8 mg/cm^2. After the catalyst loading, the electrodes were cured at 80^oC for 2 h. The Nafion® 115 membrane was boiled in 3 wt % H_2O_2 solution for 1 h. Then, it was rinsed in boiling deionized water for 2 h. In order to remove metallic contaminants on the membrane surface and exchange Na^+ for H^+ in the membrane, it was boiled in 0.5

M H_2SO_4 for 1 h. Finally, it was rinsed again in boiling deionized water for 2 h. The pretreated membrane and electrodes of a 1 cm^2 cross-sectional area were bonded together by hot pressing them under 70 kgf cm^{-2} for 90 s, maintaining the temperature at 120^oC.

Bevers et.al. (1998) developed a rolling process for the production of electrodes. Simply, the components of the catalyst layer; Pt/C catalyst and PTFE powder were mixed in a fast running knife mill. Then, the mixture was applied to the membrane by passing the catalyst applied membrane through rollers. As a gas diffusion medium pre-treated carbon clothe was applied to the catalyst coated membrane.

Passalacqua et.al. (2001) studied the effect of the Nafion content on the performance of the PEM fuel cells. The electrodes were prepared by a spraying procedure on a carbon paper substrate. A diffusion layer of Vulcan XC-72 (Cabot) and 20 wt% PTFE was sprayed on the carbon paper, and heat-treated at 350°C. The catalytic layer was prepared using 20 wt% Pt on Vulcan XC-72 catalyst mixed with a 5% Nafion solution, glycerol and ethanol and sprayed on the diffusion layer. The electrodes obtained were dried at 70°C. The Pt content was maintained constant at about 0.1 mg cm^2 for both anode and cathode, and the Nafion mixed with the catalyst was about 1 mg cm^2 without further addition of Nafion on the electrodes surface.

Sasikumar et.al. (2004) also applied well-known techniques while preparing MEAs. The electrocatalyst used for the preparation of electrode was 20 wt % Pt on Vulcan XC-72, with a surface area of 100m^2/g. A 5 wt % Nafion solution was used as the binder in the catalyst layer. The Nafion content was checked by evaporating a known volume of the solution to dryness. For the preparation of the electrode, the required quantity of 20 wt % Pt/C was placed in a beaker and wetted with a few drops of water. The required quantity of 5 wt % Nafion solution and isopropyl alcohol were added and ultrasonicated for 30 min. The catalyst ink thus obtained was coated on the gas-diffusion media by a brush method and dried at 80 ^oC for 30 min. Nafion 115 and Nafion 1035 membranes were boiled in 3% hydrogen peroxide to remove any organic impurities, washed with

water, and then boiled in 1M sulfuric acid to remove any metallic impurities as well as to convert the membrane fully to the H^+ form. Finally, it was boiled in distilled water. The MEA was prepared by placing two electrodes, with the same platinum loading on both sides of a Nafion membrane and hot pressing at 130 ^oC and 1000 psig for 2 min.

2.7. Electrochemical Measurement of the Performances of the MEAs in a PEM Test Fuel Cell

There are lots of test procedures suggested for the evaluation of the MEA performance. The performance of a MEA is determined by either the fabrication method or the operating parameters set to the test station even beside the obvious factors like the amount and the activity of the catalyst, proton conductivity of the membrane, gas diffusion layers. There is no standard testing procedure for the determination of the MEA performance currently. Therefore, the operating parameters and sequence depend on the researchers. An appropriate testing procedure must be defined and applied for the reliable electrochemical measurement of the performance a MEA.

Lalande et.al. (1995) performed the measurements at test cell temperatures of 23, 50 and 80^oC with a test fuel cell having a 5 cm^2 active electrode area for the electrochemical measurements of the MEA manufactured with tetracarboxylic cobalt phthalocyanine cathode catalyst. The anode (hydrogen) and cathode (oxygen) pressures were set to 30 and 60 psig, and the gas flow rates were set to 150 and 250 cm^3/min, respectively. In order to supply humidity, de-ionized water gas bubblers were heated to 50, 70, 105 ^oC for operating temperatures of 23, 50, 80 ^oC, respectively. Prior to polarization measurement, the fuel cell was left under open circuit for 1 hour. In another study which is conducted by Lalande et.al. (1996) the tests of the MEAs manufactured with iron phthalocyanines were conducted, a test fuel cell having 1 cm^2 active electrode area kept at 50 ^oC. The water bubblers are kept at 75 ^oC. The hydrogen and oxygen flow rates were set to 95 and 100 cm^3 and kept at pressure of 30 and 60 psig, respectively. Before making measurements, the fuel cell was kept at open circuit condition for 1 hour.

Lefévre et.al. (2000) made measurements similar to Lalande et.al. (1996) with perylene tetracarboxylic dianhydride as cathode electrocatalyst. Although the operating temperatures and pressures are the same as Lalande et.al. (1996), the flow rate of O_2 and H_2 were 360 and 230 cm^3/min.

The importance of the effect of the operating parameters on the performance of the PEM fuel cells was realized in the last few years. Experiments with different fuel cell operating temperatures, different cathode and anode humidification temperatures, different operating pressures, and various combinations of these parameters have been carried out (Wang et.al., 2003). A systematic test procedure was applied for each experiment by using a commercial test station. Tests were conducted with 50 cm^2 single test PEM fuel cell with 0.4mg Pt/cm^2 MEAs. Anode line was purged with nitrogen prior to hydrogen feed in order to prevent from combustion in the anode. The test parameters were set in the interface software. The time delay between two measurement points for the polarization curves was selected as 200s in order to ensure pseudo steady state conditions. The flow rates of hydrogen and air were 1200 and 2200 cc/min for the anode and cathode, respectively. There is no 1 h operation at open circuit voltage (OCV) conditions prior to measurements. Contrarily, the full hydration of the membrane was ensured at higher current densities which increase effective active area.

The enhancements in the test procedures should be applied to the metalo phthalocyanine based cathodic catalysts. Even for the platinum catalysts the performance can be improved by MEA manufacturing process and testing procedure and operating conditions. Therefore, the latest developments in these fields may improve the fuel cell performance assembled with Co, Fe or Ni phthalocyanines.

CHAPTER 3

EXPERIMENTAL

3.1. Materials

The materials used in this study are required either for the synthesis of metalo phthalocyanines, the preparation of catalyst, the treatment of proton conducting membrane or the preparation of membrane electrode assemblies (MEAs). Sulfuric acid, 2-propanol, phthalic anhydride, urea, nitrobenzene, nickel powder, hydrogen per oxide, ammonium molybdate, cobalt (II) chloride, iron (II) chloride, and cyanuric acid were purchased from Merck. As supporting material, carbon black (Vulcan XC-72, Cabot) was used. Membrane (Nafion® 112) and 5% Nafion® solution were obtained from Ion Power Inc. 20% Pt on carbon (E-tek). Gas diffusion layer was purchased from Sigracet® GDL 31 BC (SGL Carbon). The distilled water was obtained by distilling the tap water by the use of a water distillation apparatus (Nüve NS 108).

Gases used are nitrogen (99.999% pure) from HABAŞ (Turkey), hydrogen and oxygen (99.9999% pure) from BOS (Turkey).

3.2. Synthesis and Characterization of Metalo Phthalocyanines

The synthesis of cobalt, iron and nickel phthalocyanines were carried out by the method explained by Segawa et.al. (1990). The reaction scheme of the phthalic anhydride-urea process is given in Figure 3.1.

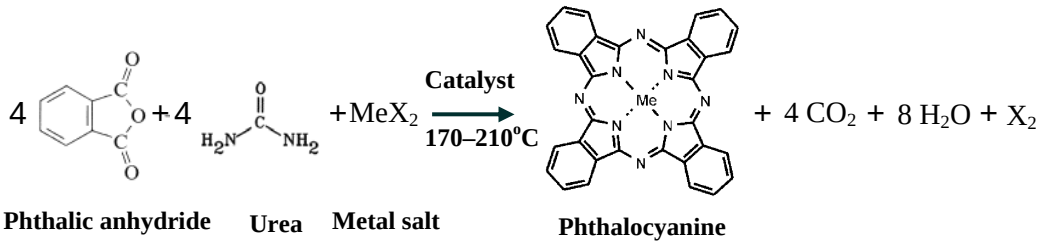

Figure 3.1 Reaction scheme of metalo phthalocyanine synthesis

3.2.1. Experimental Set-up for the Synthesis of Metalo Phthalocyanines

The experimental setup consists of a 250 ml three-necked glass reactor, a mechanical stirrer (Heidolph RZR 2041), an electric heater with thermostat, and a digital thermometer (Huger). The schematic diagram of the set-up for experiments is given in Figure 3.2 and the picture of the set-up can be seen in Figure 3.3.

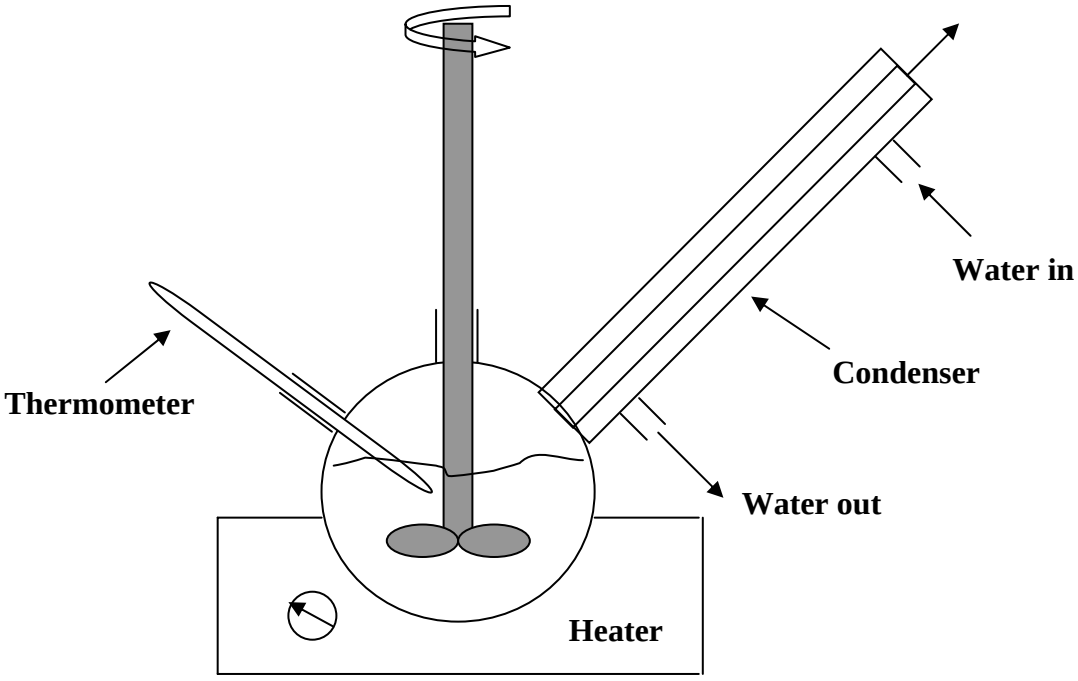

Figure 3.2 The schematic representation of the experimental set-up for metalo phthalocyanine synthesis

Figure 3.3 The picture of the experimental set-up for metalo phthalocyanine synthesis

3.2.2. Experimental Procedure for the Synthesis of Cobalt, Iron and Nickel Phthalocyanines (CoPc, FePc, NiPc)

Phthalic anhydride, urea and ammonium molybdate, cyanuric acid and nitrobenzene were charged to the three necked glass reactor shown in Figure 3.2 and Figure 3.3. For the synthesis of cobalt phthalocyanine, iron phthalocyanine, nickel phthalocyanine the material charged to the reactor were cobalt chloride 6 hydrate, iron chloride, and nickel chloride, respectively. Whereas, for the synthesis of nickel phthalocyanine, nickel powder (metal form) was used by applying the same procedure. The amounts of the material used for the synthesis are given in Table 3.1. The central neck was used for the mechanical stirrer, and to the other two necks reflux condenser and a thermometer were attached. These compounds were heated to 195 ^{o}C and kept between 190 ^{o}C and 200 ^{o}C for five hours. After 5 hours, the mixture was allowed to cool to room temperature. Then the nitrobenzene, which is the solvent of the reactants, was removed from the medium by means of vacuum distillation.

Table 3.1 The materials used for the synthesis of CoPc, FePc and NiPc

Reactants	**CoPc**	**FePc**	**NiPc**	**NiPc**
Phthalic anhydride (g)	5.402	16.21	28.32	28.32
Urea (g)	10.95	32.86	40.19	40.19
Cobalt (II) chloride-6hydrate (g)	2..17	-	-	-
Iron (II) chloride (g)	-	18.88	-	-
Nickel (II) chloride (g)	-	-	6.20	-
Nickel metal powder (g)	-	-	-	2.81
Ammonium molybdate (g)	0.040	0.12	0.11	0.11
Cyanuric acid (g)	0.70	1.22	3.40	3.40
Nitrobenzene (ml)	25.0	60.0	70	70

3.2.3. Characterization of the Metalo Phthalocyanines

The synthesized cobalt, iron, and nickel phthalocyanines were characterized by infrared spectrometry (Hitachi 270-30). Also, X-ray spectrometer (Philps PW1729) with Cu-Kα radiation was used for the characterization of cobalt phthalocyanine.

3.2.4. Thermal Gravimetric Analysis (TGA) of Metalo Phthalocyanines

The thermal behaviors of the synthesized cobalt, iron, and nickel phthalocyanines were investigated by a thermal gravimetric analyzer (General V4.1C DuPont 2000). The samples were heated at 10 ^{o}C ramp from room temperature to 1100 ^{o}C in a 100 cc/min nitrogen flow and weight loss was recorded.

3.3. Catalyst Preparation with Metalo Phthalocyanines and their Characterization

The catalyst preparation with cobalt, iron or nickel phthalocyanines was performed in two stages. First, the metalo phthalocyanines are impregnated on the carbon black (Vulcan XC-72, Cabot) support. Then, heat-treatment procedure applied to metalo phthalocyanine impregnated catalysts in order to increase both activity and stability. The flow chart for the catalyst preparation process is shown in Figure 3.4.

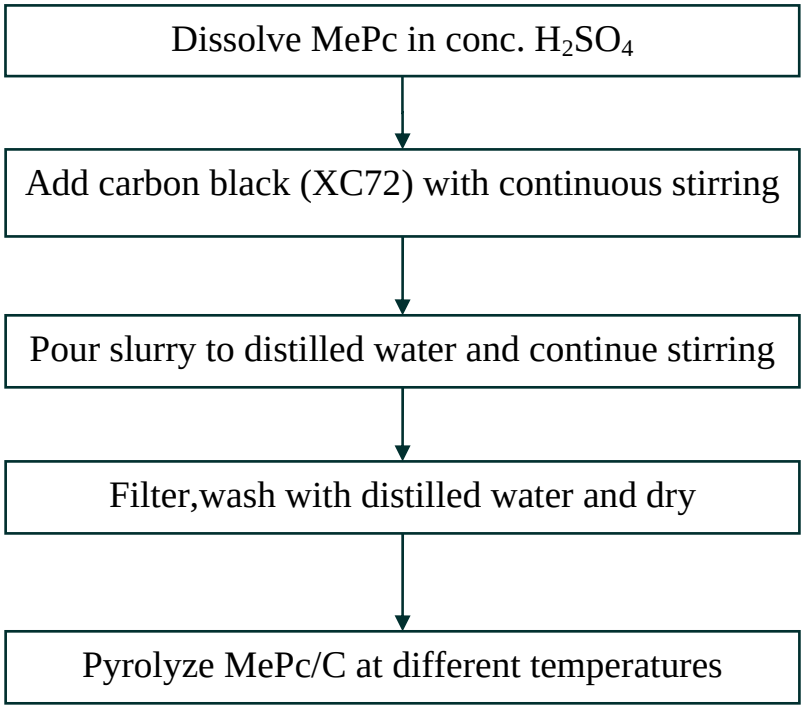

Figure 3.4 Flow chart for the catalyst preparation

3.3.1. Impregnation of Metalo phthalocyanines to Carbon Support

Various catalysts were prepared either containing 4% cobalt, 4% or 10% iron or 4% nickel phthalocyanines on carbon black (Vulcan XC-72, Cabot) matrix by the impregnation method. The amounts of the phthalocyanine compounds and carbon black used are given in Table 3.2. Sulfuric acid was used in order to dissolve CoPc and FePc (Kalvelage et.al., 2000). Carbon black was added after all of the phthalocyanines were dissolved and stirred ultrasonically (SONOREX RH 100H) for 4-5 hours. Then, the slurry was poured into distilled water portionwise that results metalo phthalocyanines

precipitated on the pores of carbon black and filtered and washed with distilled water. Resulting precipitate was dried in vacuum oven at 70°C. These catalysts were directly used for the unpyrolyzed catalyst measurements.

Table 3.2 The amount of materials used for the preparation of impregnated catalysts

	Phthalocyanine (CoPc, FePc or NiPc)	Vulcan XC-72
4% Co containing CoPc/C	1.0 g	2.47 g
4% Fe containing FePc/C	0.81 g	2.0 g
10% Fe containing FePc/C	1.02 g	1.0 g
4% Ni containing NiPc/C	0.78 g	2.0 g

3.3.2. Pyrolysis (Heat-Treatment) of Impregnated Catalysts

In order to increase the catalytic activity and stability, the metalo phthalocyanine impregnated catalysts were heat-treated. In order to carry out pyrolysis, a tube-furnace (Heraeus, Germany) capable of raising temperatures 1000 ^{o}C or above was used. The temperature of the tube-furnace was controlled by a microprocessor based controller (GEMO DT442) and a K-type thermocouple. The flow rate of the inlet nitrogen gas was measured by a Rota meter. The tube was made of quartz. The schematic representation and the picture of the pyrolysis set-up are given in Figure 3.5 and Figure 3.6, respectively. CoPc/C and NiPc/C catalysts were pyrolyzed at either 600°C or 1000°C and FePc/C catalyst was pyrolyzed at 1000°C in a tube furnace under 0.1 L/min nitrogen flow. Heating rate of the furnace was kept at 10°C/min. The furnace was kept at set value for 20-30 minutes. Then the furnace was let to cool down to the room temperature under nitrogen flow.

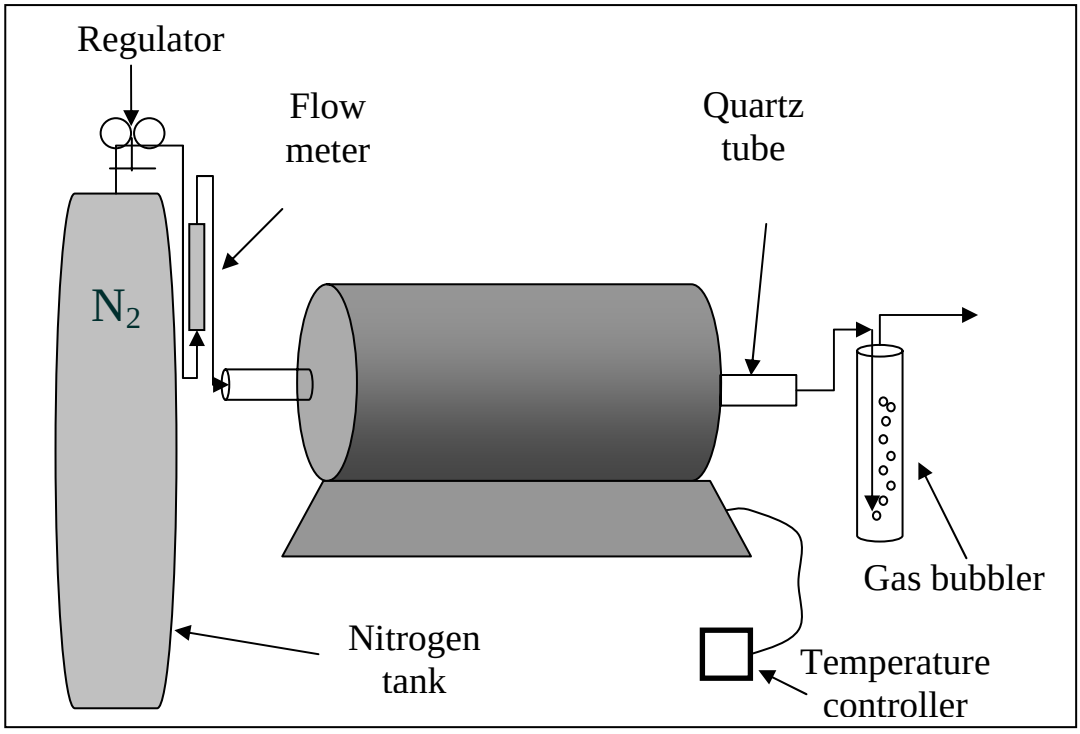

Figure 3.5 The schematic representation of the experimental set-up for pyrolysis

Figure 3.6 The picture of the experimental set-up for pyrolysis

3.3.3. Characterization of Impregnated and Pyrolyzed Catalysts by Scanning Electron Microscopy

The characterization of the impregnated and/or heat treated catalyst samples were achieved by an Electron Microscope (JEOL JSM-6400, METU), equipped with NORAN System 6 X-ray Microanalysis System & Semafore Digitizer.

3.3.4. Analysis of the Pore Structures

The BET surface area and pore size distribution of the carbon black and catalysts prepared with impregnating cobalt or iron on carbon black support were analyzed by using a commercial volumetric gas adsorption apparatus (ASAP 2000, Micromeritics Co).

BET areas of the samples were obtained by nitrogen gas adsorption and desorption isotherms at 77 K. The area and the volumes of the pores as well as their distributions were evaluated from the nitrogen adsorption isotherms using the Barrett, Joyner and Halenda (BJH) method by using the available software.

3.4. Preparation of Electrodes and Membrane Electrode Assemblies (MEA)

The anode electrode in all the cases was prepared with 0.4 mg Pt/cm^2 having 20% Pt/C catalyst. The cathode was manufactured by using the CoPc/C, FePc/C or NiPc/C either unpyrolyzed or pyrolyzed. The catalyst ink was prepared from 0.12 g 5% Nafion® solution, 1:7 ratio of distilled water to 2-propanol, either Pt or MePc catalyst by mixing in an ultrasonic mixer for 1-2 hours, as suggested by Passalacqua et al., (2001).

Gas diffusion layers were coated with the catalyst ink by spraying technique. A pneumatic spray gun was used for coating the catalyst to the hydrophobically treated layer of the gas diffusion media. Once a single ultra thin layer was coated, the surface was dried by a hot air gun set at 80 ^{o}C. This coating-drying cycle was repeated many

times. The catalyst coated gas diffusion layer (GDL) was weighted in order to determine if the desired catalyst load was reached or not. When the desired load was reached for anode and cathode, the catalyst coated GDLs were hot pressed onto the both sides of the Nafion membrane which was treated as described in Figure 3.7. The MEA manufacturing process is summarized in Figure 3.8.

Nafion® 112 membrane was conditioned prior to assemble of catalyst coated gas diffusion layers as described in the flow chart in Figure 3.7. 3% H_2O_2 solution, distilled water and 0.5 M H_2SO_4 kept in water bath at 80°C (Qi and Kaufman, 2002). Membrane was immersed sequentially into H_2O_2, distilled water, H_2SO_4 and the distilled water again, respectively for 1 hour of each. After drying the membranes, the electrode-applied gas diffusion layers were pressed at 130°C and 1000 kgf for 3 minutes. Then, the press was released, the membrane electrode assembly (MEA) was removed from the hot plate and let it to cool down to room temperature.

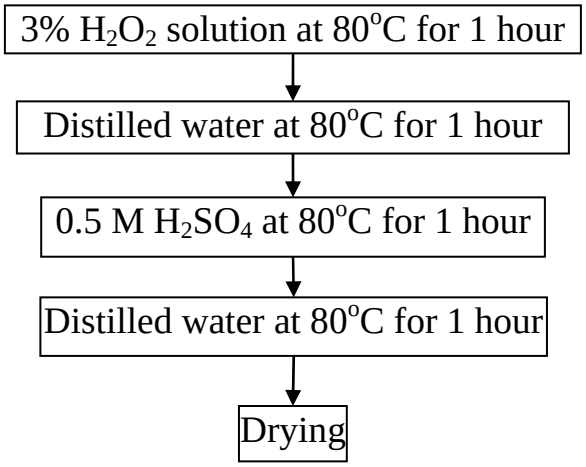

Figure 3.7 The flow chart for the membrane treatment process

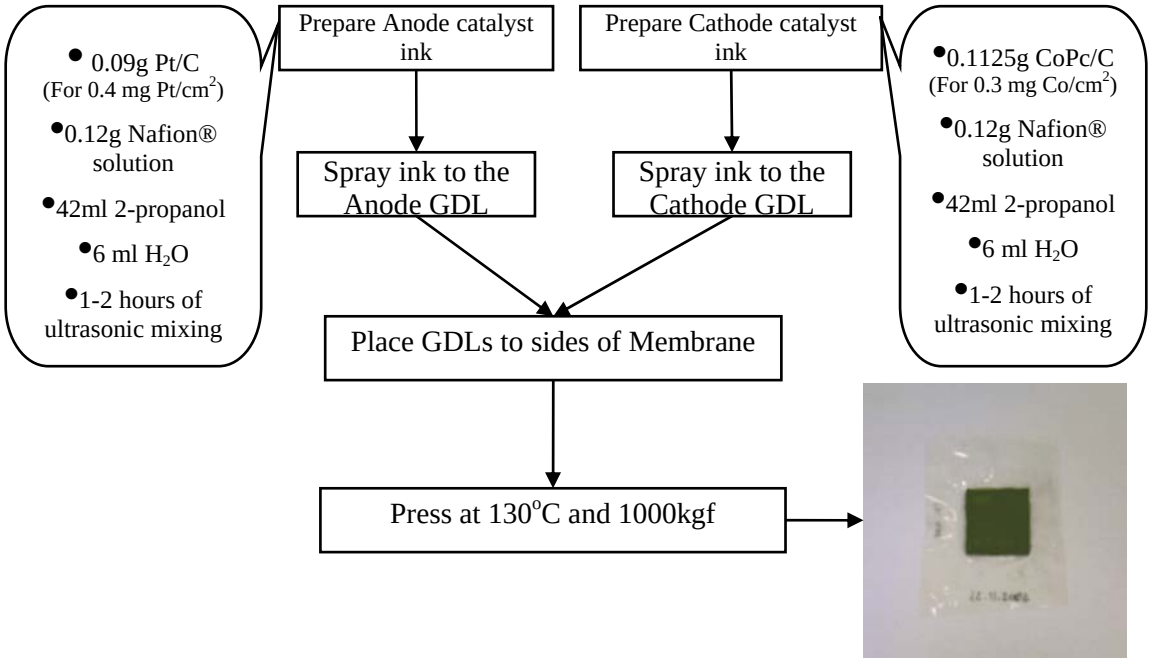

Figure 3.8 Manufacturing process for the membrane electrode assembly (MEA)

3.5. Performance Measurements

3.5.1. PEM Fuel Cell Test Station

Performance measurements of the manufactured MEAs were carried out with the PEM fuel cell test station built at METU Fuel Cell Technology Laboratory. A schematic representation and a picture of the test station are given in Figure 3.9 and Figure 3.10, respectively. The test station is capable of testing single PEM fuel cells and small PEM fuel cell stacks with one oxidation gas and up to three gas mixtures as a fuel. For that purpose the test station was equipped with four mass flow controllers (MFCs). The cathode MFC (Aalborg GFC171) was chosen for pure oxygen and it was factory-calibrated. Each anode fuel MFCs (Aalborg GFC171) were also factory-calibrated specially for hydrogen, carbon dioxide and carbon monoxide. That is, the test station is capable of running on reformat simulation. However, throughout the experiments

performed test station was run on pure hydrogen fuel mode. The piping from high pressure gas cylinders to fuel cell was made of 6mm OD stainless steel pipes. Bubble type humidifiers that were made of stainless steel, were built in order to supply reactant gases to the fuel cell in the desired humidity level. Each humidifier were equipped with 200 W resistant heaters and thermally insulated. The temperature of the each humidifier can be controlled by a PID temperature controller (GEMO DT442) and K-type thermocouple individually. In order to prevent the condensation, the gas transfer lines between the humidifiers and the test fuel cell were built with electrical-resistive-heaters. That is, the temperatures of the heated gas transfer lines were kept at a set temperature by on/off type temperature controllers.

A test PEM fuel cell having a $5cm^2$ active electrode area was used throughout the study (Electrochem FC05-01SP-REF). The exhausts of the anode and cathode were purged to the environment by passing from the gas bubblers in order to visualize the gas flow. The external load applied to the fuel cell was adjusted by an 11ohm manual type rheostat. The current and voltage of the cell were monitored throughout the operation of the cell. The current data were measured and logged by a multimeter (Brymen BM857) and a data logger program (BS85x Data Logging System Ver 5.1.0.4). The voltage of the cell was monitored and logged by A/D data logger PC card (Advantech PCL-711) and a data logger program written in Visual Basic® programming language. The Windows XP driver of the data logger A/D converter card was downloaded from the manufacturer's web site (Advantech).

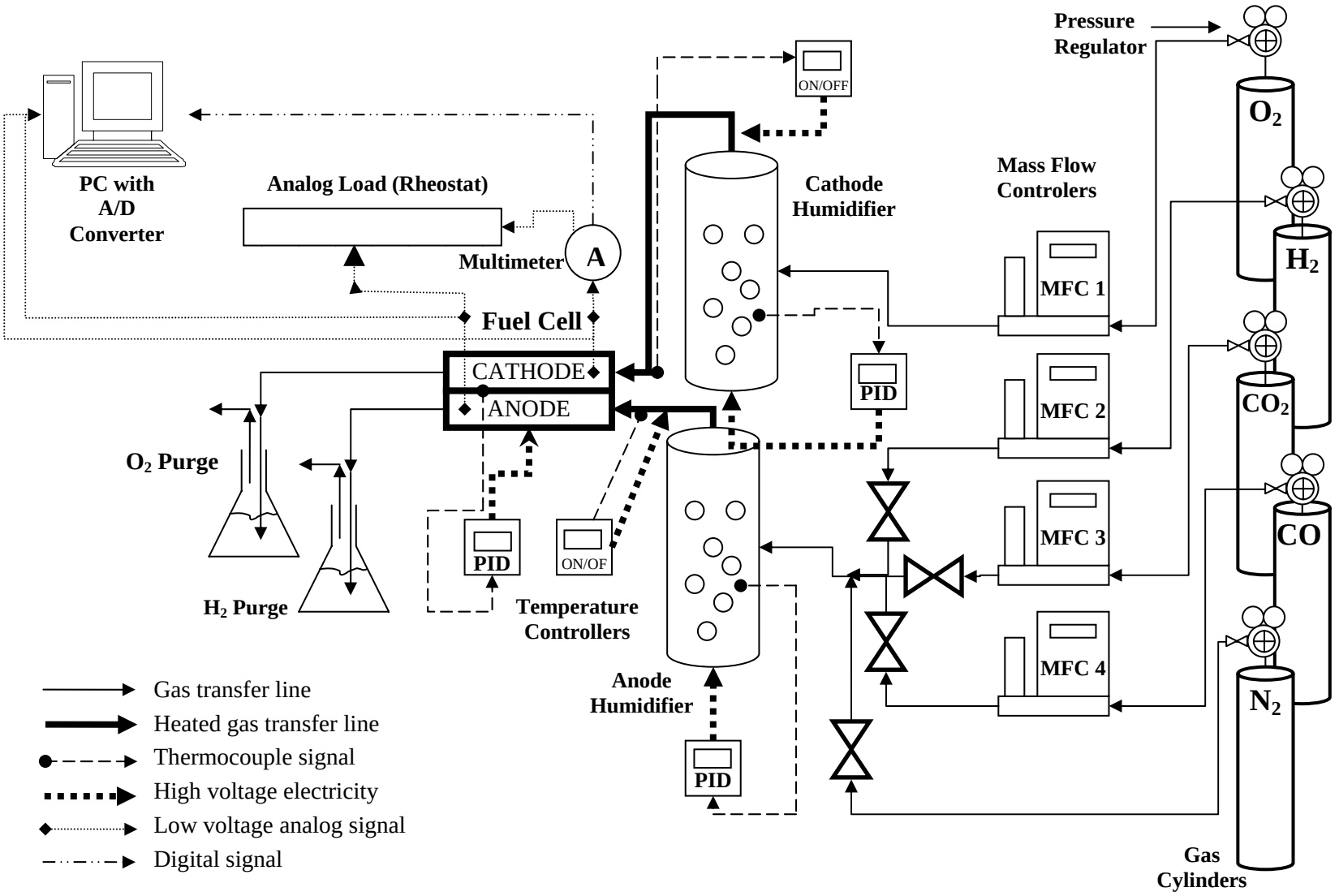

Figure 3.9 Schematic representation of PEM fuel cell test station

Figure 3.10 The picture of the PEM fuel cell test station

The screen shot of the written data logging program is given in Figure 3.11.and the code of the program is supplied in the Appendix B.

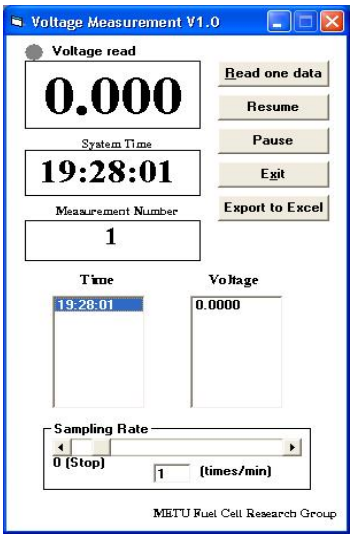

Figure 3.11 The screenshot of the voltage measurement program written in Visual Basic

3.5.2. Test Procedure of a New Assembled Test Fuel Cell

One of the membrane electrode assembly manufactured by the spraying technique was placed to the test cell and the bolts were tightened at a torque of 15-20 lb-in for each bolt. For a new assembled test cell, the following test procedure was applied at start-up. First, the anode line of the fuel cell was purged with nitrogen. If any gas leak either in the test cell or on the gas line were detected and the oxygen coming from the air was flushed so that the risk of the combustion at the anode was prevented by this procedure. Another possible problem was the bulk diffusion of the gasses across the membrane. In the case of any bulk diffusion, the combustion began immediately and the temperature of the test cell started to increase abnormously. Since the bulk diffusion occurs with the existence of a small puncture or any hole in the membrane, a testing procedure was required to detect the bulk diffusion. Therefore, the following detection procedure was applied. During the nitrogen purging period, the pressure of the nitrogen was adjusted to

0.5 bar and anode exit was blocked. The existence of the gas bubbles at the cathode purge was the sign of the hole on the membrane. When these tests were passed, the hydrogen and oxygen were fed to the fuel cell with a flow rate of 0.1 L/min.

3.5.3. Experimental Procedure for the Determination of the Polarization Curve of the Test Fuel Cell

The fuel cell was turned on by following the start-up procedure. Fuel cell and gas humidifiers were set to 55 ^{o}C. In order to prevent condensation, the temperatures of the gas transfer lines were kept at 60^{o}C. The load was adjusted to minimum resistance which causes the reaction to occur. The fuel cell was allowed to operate 5-6 hours in order to reach the steady state. The rheostat was used to change the load connected to the cell. The load resistance was increased gradually starting from the lowest resistance. At the each increment step, the load was kept constant for 3-5 minutes to reach steady state again and the voltage and current values were logged and recorded at different loads.

The polarization curves obtained were the identical performance results of the inspected membrane electrode assembly which was prepared with synthesized phthalocyanines.

3.6. Scope of the Experiments

By using the cobalt, iron and nickel phthalocyanines by changing the pyrolysis temperature the catalysts given in Table 3.3 were prepared.

Table 3.3 Scope of the catalyst preparation

	4% Me	10% Me	Unpyrolysed	Tp=600^{o}C	Tp=1000^{o}C
CoPc/C	✓	-	✓	✓	✓
FePc/C	✓	✓	✓	-	✓
NiPc/C	✓	-	✓	✓	✓

While preparing the catalysts given in Table 3.3., the following parameters were kept constant:

- The flow rate of the nitrogen used in the pyrolysis (100 cc/min)
- The ramp of the heating (10 ^{o}C/min)

MEAs were prepared by using commercial 20% Pt containing Pt/C catalysts for the anode and the prepared catalysts for the cathode. Anode metal loading was kept constant as 0.4 mg Pt/cm^2 throughout the experiments. The cathodes were prepared as summarized in Table3.4. Percentage of the cobalt, iron or nickel phthalocyanines on carbon black support means that the 4% or 10% of the unpyrolyzed catalyst is cobalt, iron or nickel. Needless to say, the metals are not in their metallic form, but in the molecular structure of phthalocyanines.

Table 3.4 The cathode catalysts of the manufactured membranes

	mg Metal/cm^2	4% CoPc/C	4% FePc/C	10% FePc/C	4% NiPc/C	20% Pt/C
MEA1	0.30	0^{o}C	-	-	-	-
MEA2	0.30	600^{o}C	-	-	-	-
MEA3	0.28	1000^{o}C	-	-	-	-
MEA4	0.14	1000^{o}C	-	-	-	-
MEA5	0.30	-	0^{o}C	-	-	-
MEA6	0.30	-	1000^{o}C	-	-	-
MEA7	0.30	-	-	1000^{o}C	-	-
MEA8	0.30	-	-	-	0^{o}C	-
MEA9	0.30	-	-	-	600^{o}C	-
MEA10	0.30	-	-	-	1000^{o}C	-
MEA11	0.4	-	-	-	-	As purchased

The operating conditions of the test station were kept constant throughout the experiments as listed below:

- The temperature of the single PEM fuel cell (T_{cell}=55^{o}C)
- The temperature of the heated gas transfer lines (T_{gtl}=60^{o}C)
- The temperature of the anode and cathode humidifiers (T_{ah}=T_{ch}=55^{o}C)
- The flow rates of the hydrogen and oxygen (Q_{H_2}=Q_{O_2}=0.1 slm)

CHAPTER 4

RESULTS AND DISCUSSION

4.1. Characterization of Cobalt, Iron and Nickel Phthalocyanines

4.1.1. Characterization by Infrared (IR) Spectrometry

The synthesized cobalt, iron and nickel phthalocyanines were characterized by infrared spectra. Infrared spectrometry is a great tool for the determination of an unknown sample. The spectrum obtained for the cobalt phthalocyanine by the infrared spectrometer is given in Figure 4.1.

One may approach in two different ways in order to analyze the sample with this method. In the first case, the sample is unknown and there is no idea about what the sample is. The wave numbers of the peaks must be listed and the chemical bonds and functional groups corresponding to each wave number must be determined. According to this information, the unknown sample might be determined. In the second case, the sample is probably a known material. Then, the infrared spectrum of the suspected material may be compared with the infrared spectrum of the sample. Since the infrared spectrum of a material is like the “fingerprint” of the material, the materials are the same if two infrared spectra coincide with each other.

The infrared spectrum found from the literature was edited and cut from the original image by using a photo editing program (Adobe Photoshop) and pasted into the

spectrum generated by the infrared spectrometer for the sample. The upper spectrum in Figure 4.1 shows the infrared spectrum of the cobalt phthalocyanine found in the website of National Institute of Advanced Industrial Science and Technology (AIST), Japan. The original infrared spectrum for CoPc is given in Figure A.1.

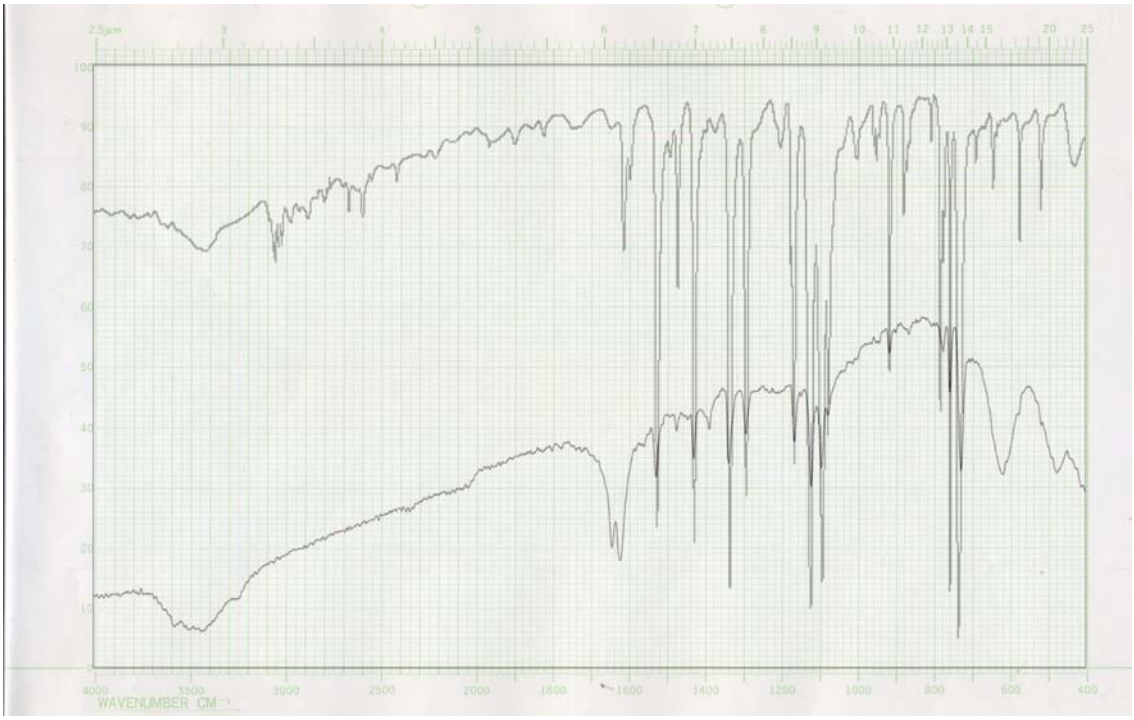

Figure 4.1 The comparison of infrared spectrum of the synthesized cobalt phthalocyanine (bottom) with the IR spectra found in the literature (top).

The peaks of the both infrared spectra coincide with each other for the wave numbers below 1700 cm^{-1}. Thus, we can conclude that the material synthesized was CoPc.

The iron phthalocyanine sample was also applied to the same characterization procedure as cobalt phthalocyanine and Figure 4.2 was obtained. The peaks of the both infrared

spectra coincide with each other for the wave numbers less than 1800 cm^{-1} except the peak at 900 cm^{-1}. The peak existing in the literature data was not seen in the spectrum for the synthesized iron phthalocyanine sample. This may be due to an experimental error occurred if the spectral database is indubitable. The physical properties of the product such as color, resistance to organic solvents were also supported the sample to be iron phthalocyanine.

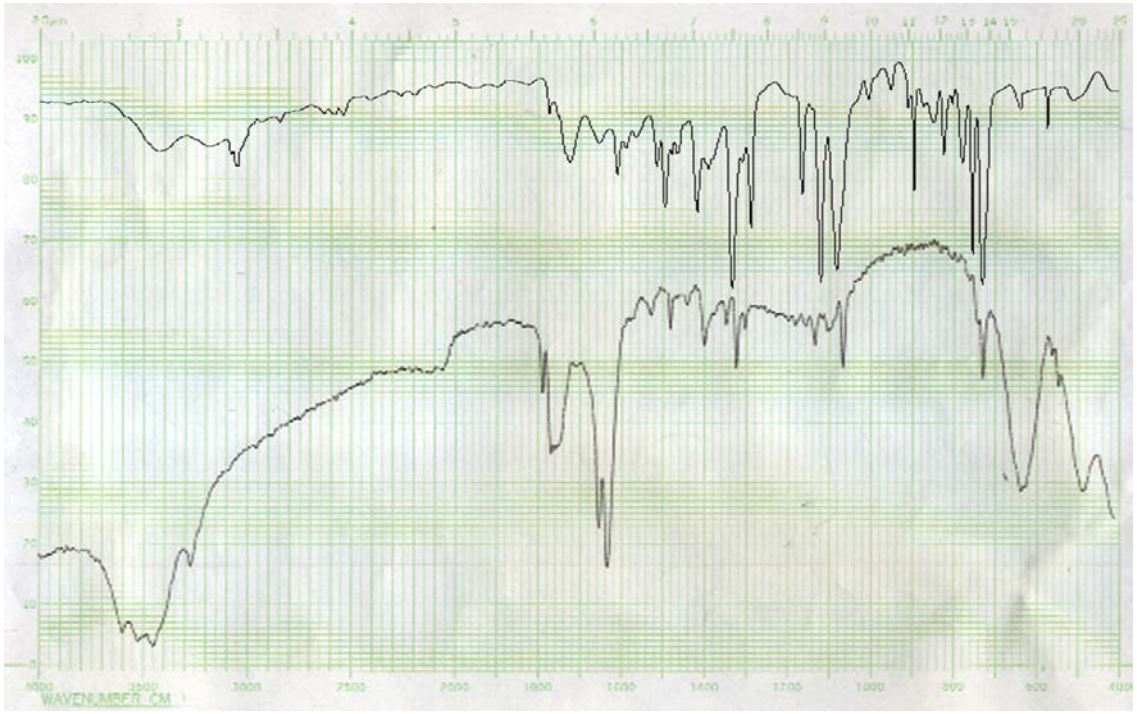

Figure 4.2 The comparison of infrared spectrum of the synthesized iron phthalocyanine (bottom) with the IR spectrum found in the literature (top).

The same characterization technique was also applied to the nickel phthalocyanines synthesized. Figure 4.3 consists of the infrared spectrum of the nickel phthalocyanine found in the literature on the bottom, nickel phthalocyanine sample synthesized (by

nickel chloride with phthalic anhydride-urea method in the middle and nickel phthalocyanine sample synthesized by nickel powder with phthalic anhydride-urea method) on the top. Two infrared spectra for the synthesized NiPc samples had exactly the same absorption frequencies. Moreover, the spectrum found from the literature has the same identical peaks at the “fingerprint” region. This result also indicates that the starting material might be both the salt of the metal or the metal itself might be used for the synthesis reaction.

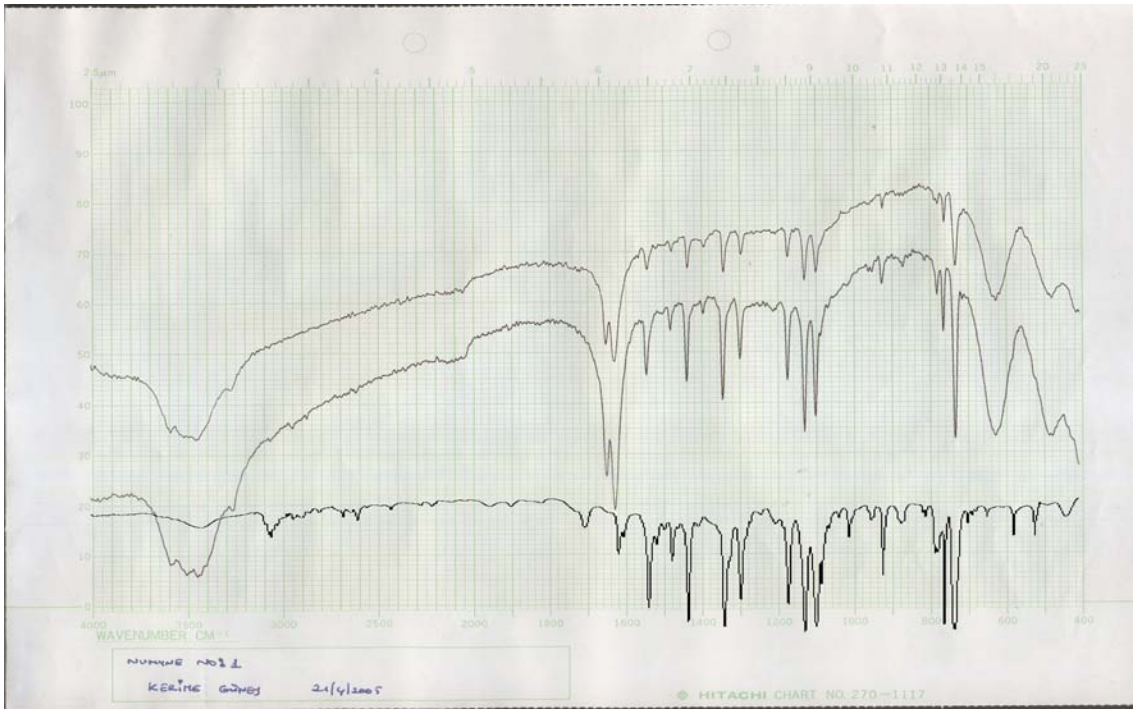

Figure 4.3 The comparison of infrared spectrum of the synthesized nickel phthalocyanine with the IR spectrum found in the literature

4.1.2. Characterization by Thermal Gravimetric Analysis (TGA)

The thermal behavior of the cobalt, iron, and nickel phthalocyanines were investigated by thermal gravimetric analysis (TGA). The TGA result of cobalt phthalocyanine is given in Figure 4.4. Weight loss peaks were observed at 223.95, 314.09, 368.29, 644.95, 703.42, 841.88, and 1007.24 ^{o}C. The early weight loss may indicate the existence of impurities in the sample. About 30% of the starting CoPc sample was decomposed below 600^{o}C. Kalvelage et. al. (2000) were investigated the nonvolatile ingredients of the decomposition products of cobalt and iron phthalocyanines pyrolyzed at 600^{o}C and reported that 90% of the pyrolysis products is phthalimide, 8% is phthalic acid dinitrile, 1% is non-cyclic N-compounds, and 1% is the N-free compounds. More detailed work about the pyrolysis products of the cobalt phthalocyanine was carried out by Achar et.al. (2005). In that study, cobalt phthalocyanine polymer was pyrolyzed between 500 and 1000 ^{o}C and the pyrolysis products were analyzed by MS and GC-MS. The main products of the pyrolysis were reported as cyanogens $(CN)_2$, hydrogen cyanide (HCN), benzonitrile (C_6H_5CN), and phthalonitrile ($C_6H_4(CN)_2$).

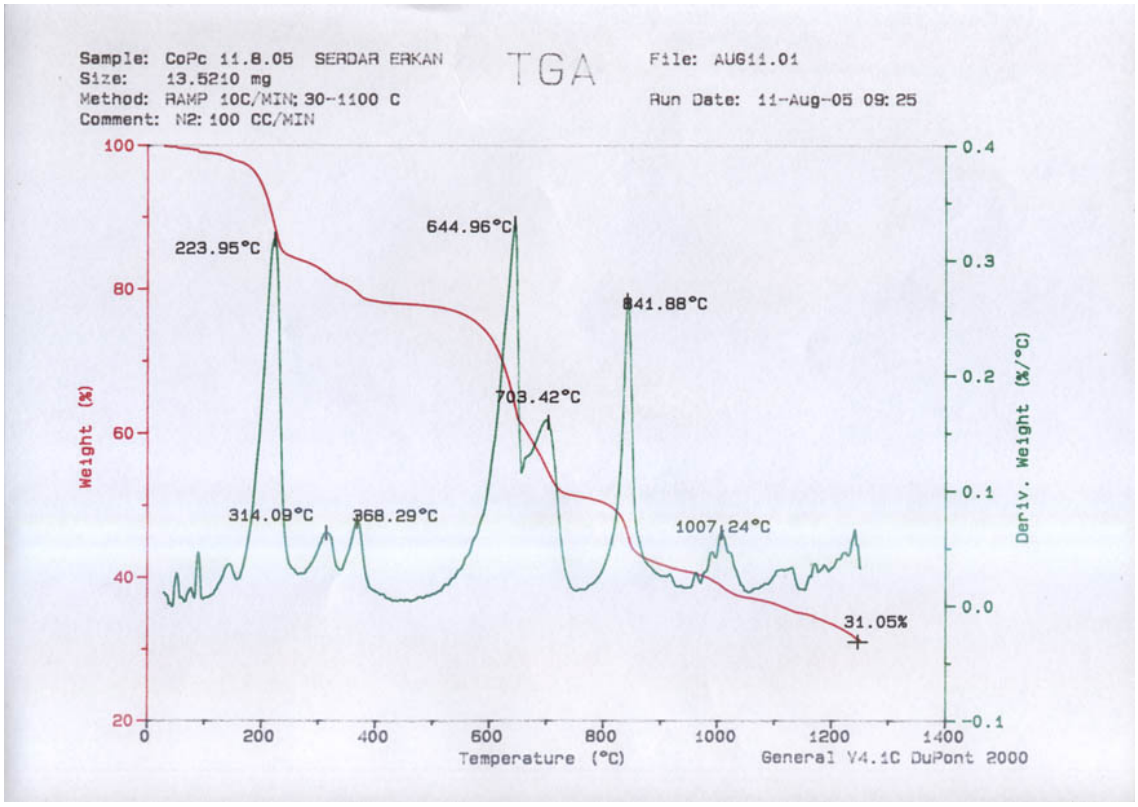

Figure 4.4 Thermal gravimetric analysis (TGA) of cobalt phthalocyanine

The TGA result of iron phthalocyanine is given in Figure 4.5. Weight loss peaks were observed at 142.47, 352.68, 462.71, 648.66, 706.99, 803.28, and 906.63 ^{o}C. About 30% of the FePc was decomposed at pyrolysis temperature of 600^{o}C. Similar to CoPc, the pyrolysis products of FePc might be 90%, phthalimide, 8% phthalic acid dinitrile, 1% non-cyclic N-compounds, and 1% N-free compounds (Kalvelage et.al., 2000). The decomposition products of $(CoPc)_n$, which were reported by Achar et.al. (2005), might be applicable in the case of FePc.

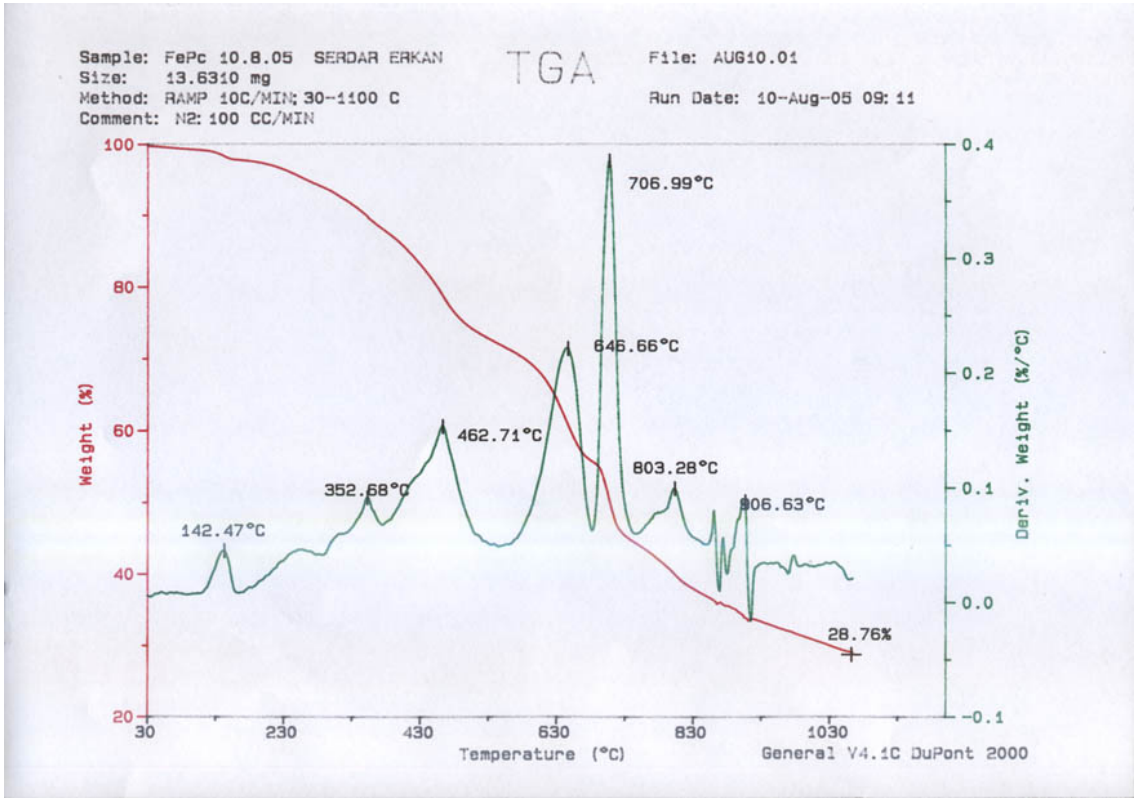

Figure 4.5 Thermal gravimetric analysis (TGA) of iron phthalocyanine

The TGA result of nickel phthalocyanine is given in Figure 4.6. Weight loss peaks were observed at 666.24 and 856.70 ^{o}C. The TGA of nickel phthalocyanine was different from cobalt and iron phthalocyanines. NiPc did not decompose until 530 ^{o}C. However, about 61% of the NiPc was decomposed at pyrolysis temperature of 700^{o}C.

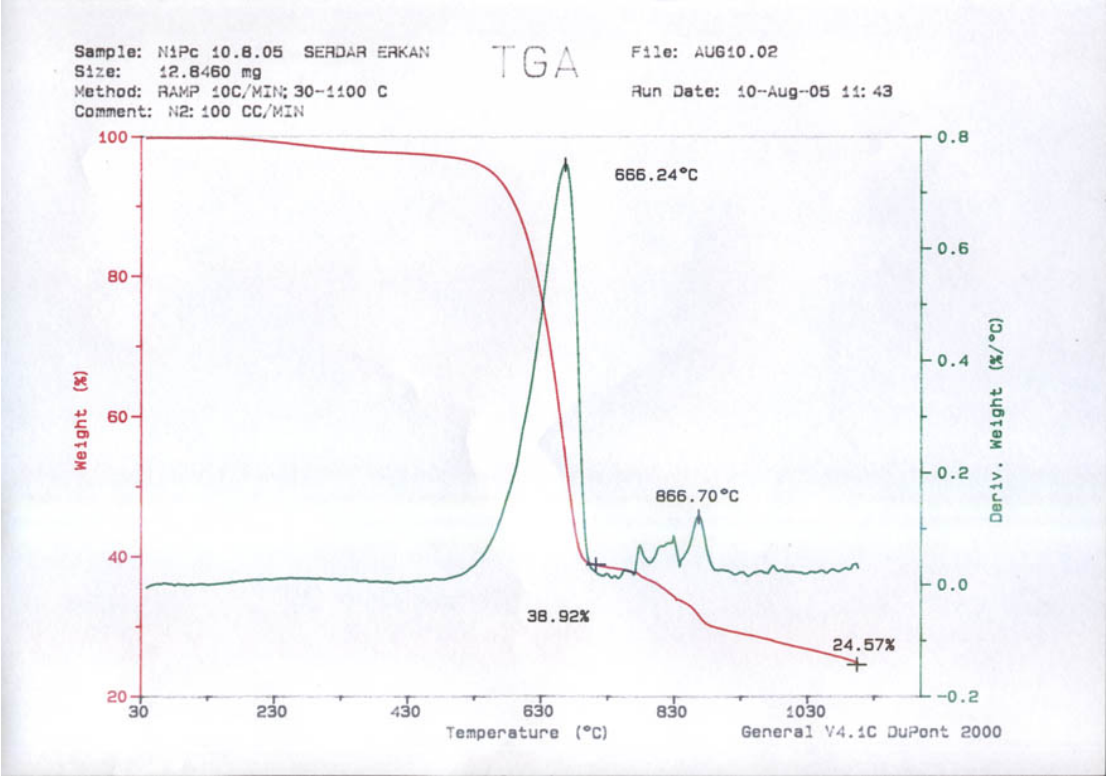

Figure 4.6 Thermal gravimetric analysis (TGA) of nickel phthalocyanine prepared by using nickel(II)chloride

4.1.3. Characterization by X-Ray Diffractometry (XRD)

X-ray Diffractometry is also an important tool for the characterization of the materials. Each crystalline solid has its unique characteristic X-ray (powder) pattern which may be used as a "fingerprint" for its identification. The X-ray pattern given in Figure 4.7 belongs to the cobalt phthalocyanine sample. The x-axis and y-axis indicate the diffraction angle (2θ) and intensity at that diffraction angle, respectively. The diffraction angle and the intensity data of CoPc was found from the literature (Powder Diffraction

File, 1989) and given in Table 4.1. The data were numbered from the highest to lowest intensity and placed to the corresponding diffraction angles in the diffraction pattern given in Figure 4.7. The base line was drawn to the diffraction pattern in order to determine the intensities of the peaks.

Table 4.1 The X-ray powder diffraction file data for cobalt phthalocyanine (Powder Diffraction File, 1989)

	$\overset{0}{A}$	2θ
1	12.4_x	7.1
2	3.20_8	27.9
3	8.79_6	10
4	5.60_6	15.8
5	3.34_6	26.7
6	3.69_3	24.1
7	3.56_3	25
8	2.93_1	30.5

Wavelength ($\overset{0}{A}$) data given in Table 4.1 was found from the literature and this data were converted to angle by using $n\lambda=2d\sin\theta$ with $n\lambda= 1.5418$ for Cu X-ray tube.

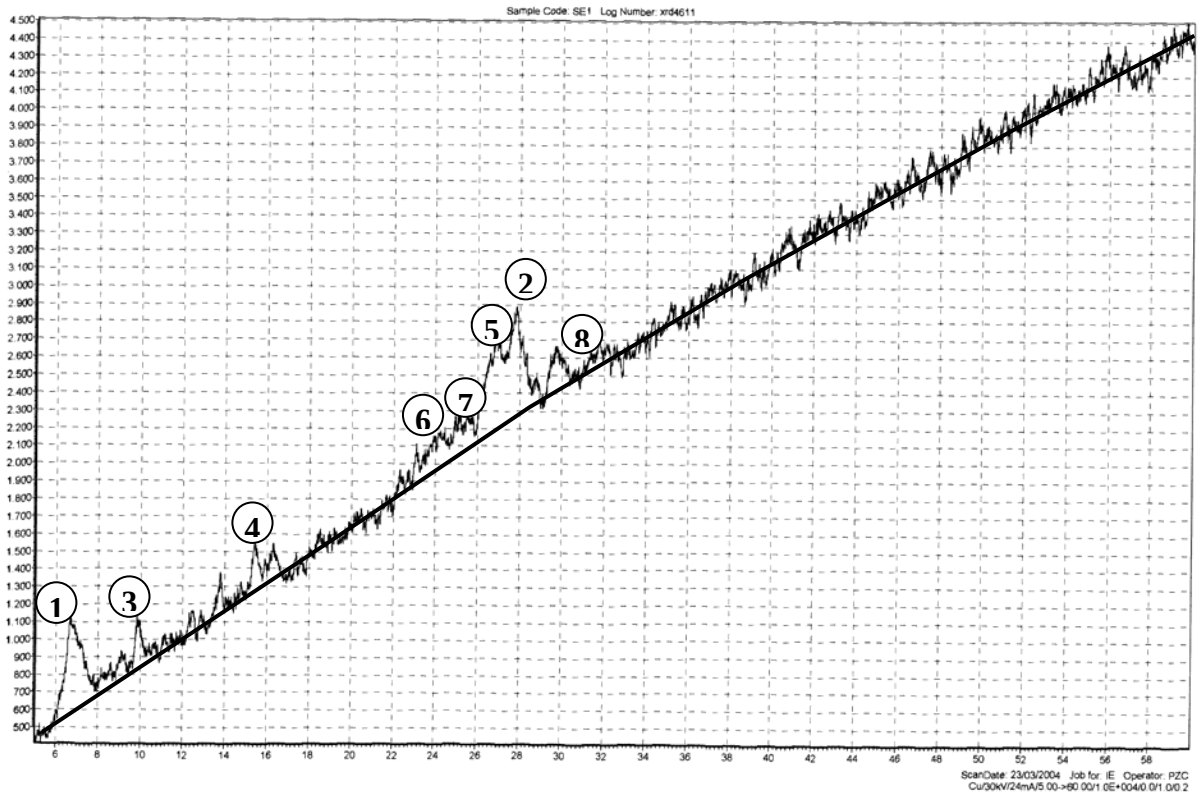

Figure 4.7 X-ray diffraction pattern of the cobalt phthalocyanine sample

4.2. Surface Morphology of Catalysts

4.2.1. SEM Micrographs and EDX Spectra of Cobalt Phthalocyanine

The surface morphology of the prepared catalysts were investigated by scanning electron microscopy (SEM) and the composition of the surface elements were analyzed with energy dispersive X-ray Spectroscopy (EDXS). The SEM micrographs of CoPc impregnated on carbon black are shown in Figure 4.8 with 400 and 5000 times of magnification. In the micrograph having 400 times magnification, carbon black particles with various sizes are seen. Porous structure of the carbon black can be seen at the magnification 5000 times.

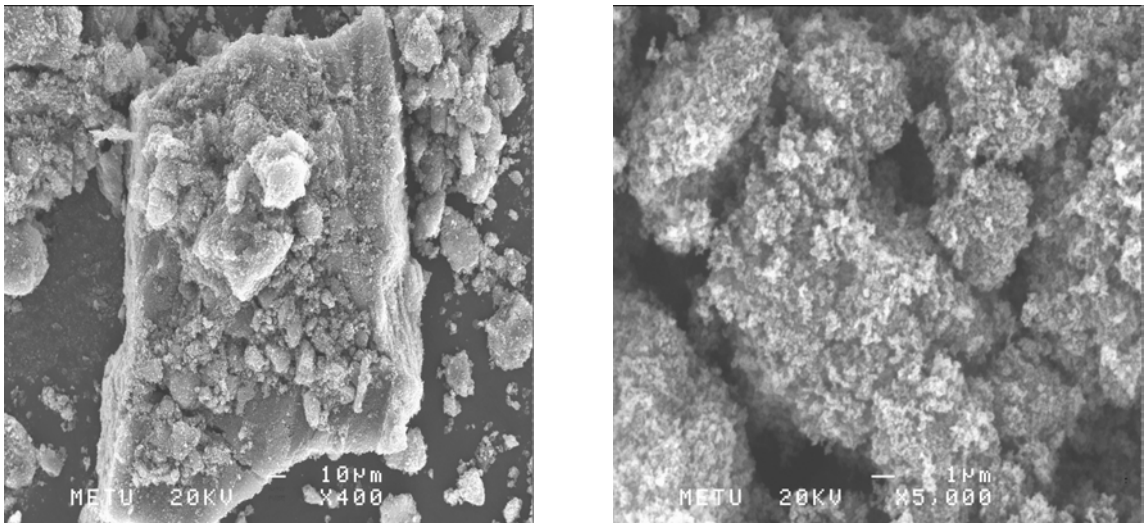

Figure 4.8 SEM micrographs of the CoPc impregnated on carbon black

The surface composition of the unpyrolized CoPc/C illustrated in Figure 4.9 was obtained by EDX spectroscopy. As it was expected, the highest peak was observed for carbon since it was used as supporting material for the catalyst. The ratio of cobalt to carbon was about 0.04 which was also an expected value. The gold peaks in the EDX spectra of the catalyst sample are due to the gold coating used during the specimen preparation step. The existence of the sulfur peak was supposed to be due to the sulfuric acid which was used as a solvent in the impregnation process. Although the impregnated catalyst was washed repeatedly by using distilled water, some amount of sulfuric acid seems to be adsorbed on the carbon black and could not been removed.

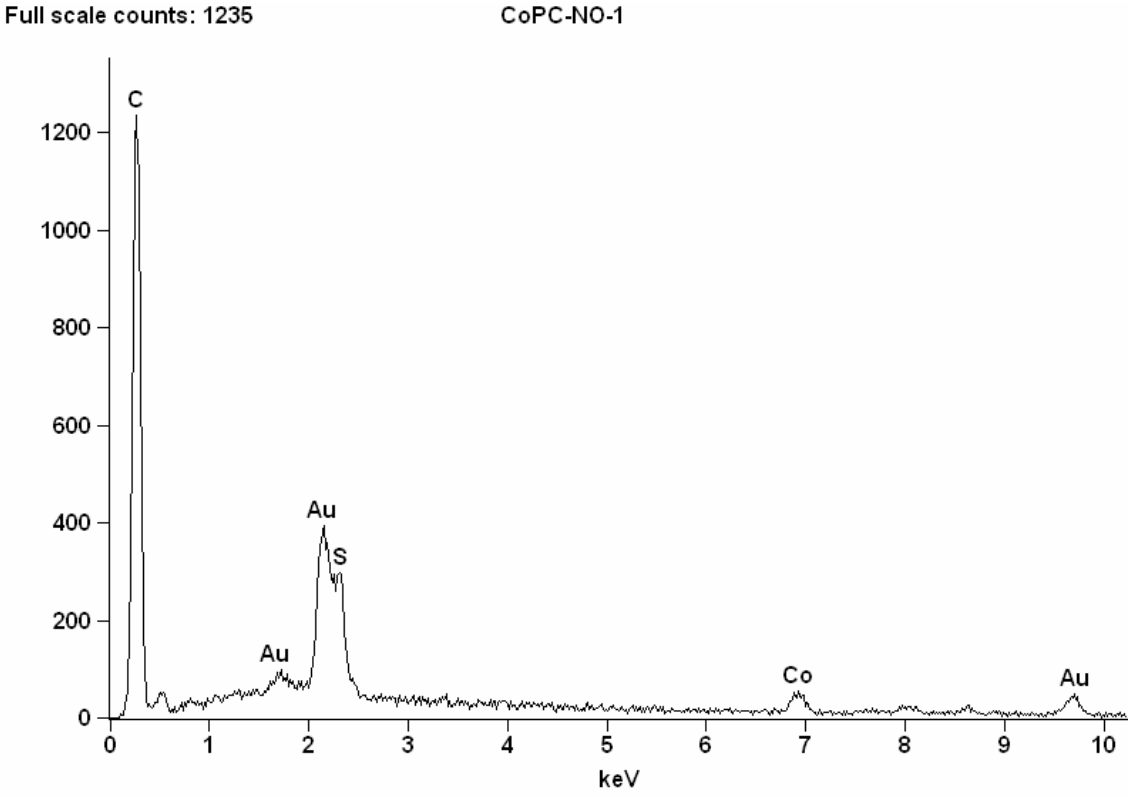

Figure 4.9 EDX spectra of the CoPc on carbon black

4.2.2. SEM Micrographs and EDX Spectra of Iron Phthalocyanine

The SEM micrographs of FePc impregnated on carbon black and pyrolyzed at 600^{o}C are shown in Figure 4.10 with 1800 and 5000 times of magnification.

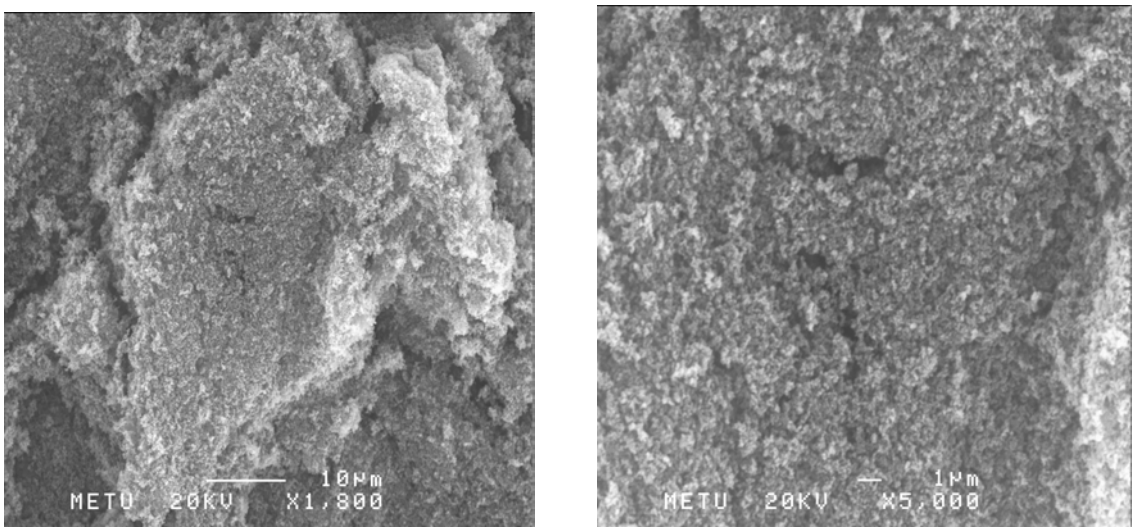

Figure 4.10 SEM micrographs of the FePc impregnated on carbon black and pyrolyzed at 600^{o}C

The EDX spectroscopy of the FePc/C pyrolyzed at 600^{o}C revealed the surface composition as illustrated in Figure 4.11. As it was expected, again the highest peak was observed for carbon since it was used as supporting material for the catalyst. The gold peaks in the EDX spectra of the catalyst sample are due to the gold coating used during the specimen preparation step. The sulfur peak was disappeared in this case. The reason of this might be the heat treatment of the catalyst. That is, the decomposition or evaporation of the sulfuric acid was resulted the removal of the sulfur atoms from the carbon catalyst support.

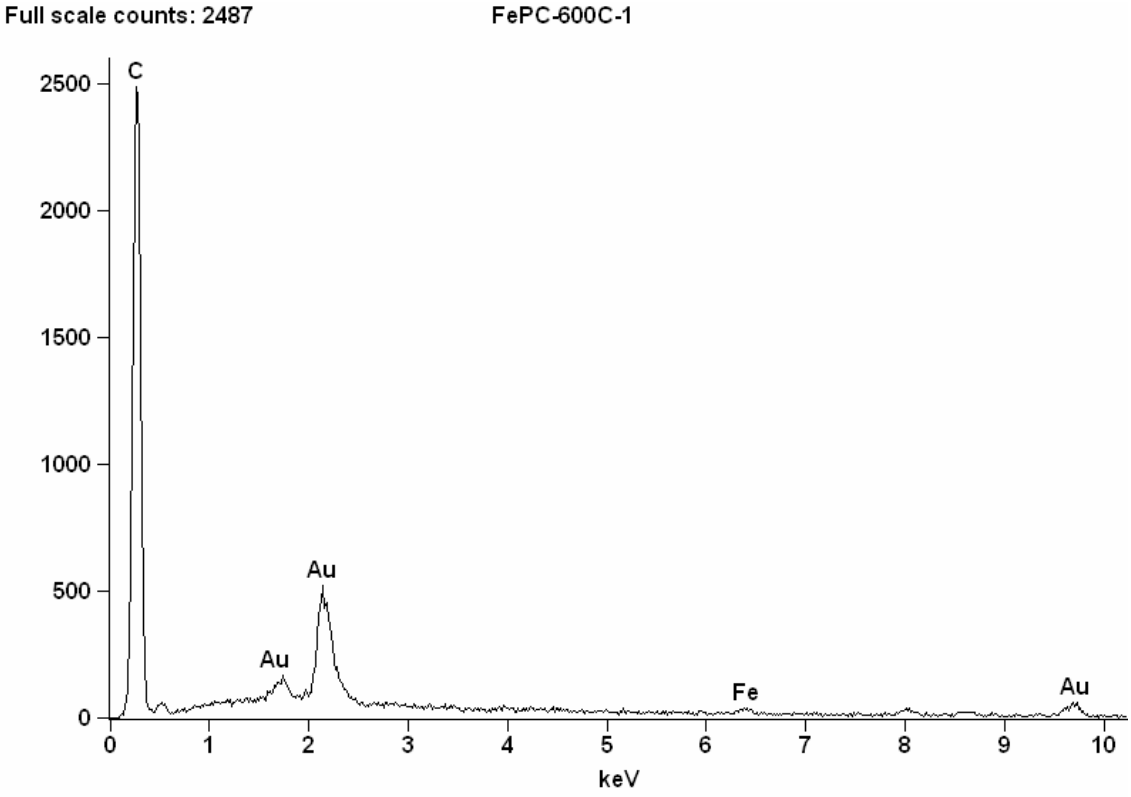

Figure 4.11 EDX spectra of the FePc impregnated on carbon black and pyrolyzed at 600^{o}C

The SEM micrographs of FePc impregnated on carbon black and pyrolyzed at 1000^{o}C are shown in Figure 4.12 with 400 and 5000 times of magnification. The increase of the pyrolysis temperature from 600^{o}C to 1000^{o}C did not result any structural change for the support pores.

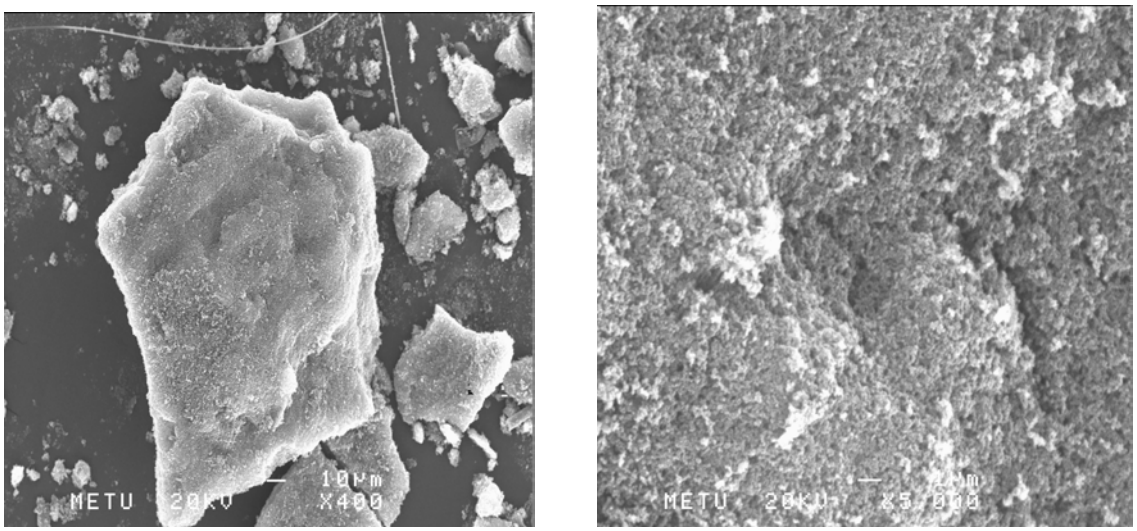

Figure 4.12 SEM micrographs of the FePc impregnated on carbon black and pyrolyzed at 1000^{o}C

The surface composition of the FePc/C pyrolyzed at 1000^{o}C illustrated in Figure 4.13 was obtained by EDX spectroscopy. As in the previous cases the EDX spectrum of the FePc/C catalyst pyrolyzed at 1000^{o}C have mainly carbon peak which is the support material and gold peaks coming from the sample preparation for the EDXS analysis. There is no sulfur atom found on the scanned surface which confirms that the decomposition of the sulfuric acid was obtained during the pyrolysis. The existence of the iron atoms on the surface is also verified by the result of EDX spectra.

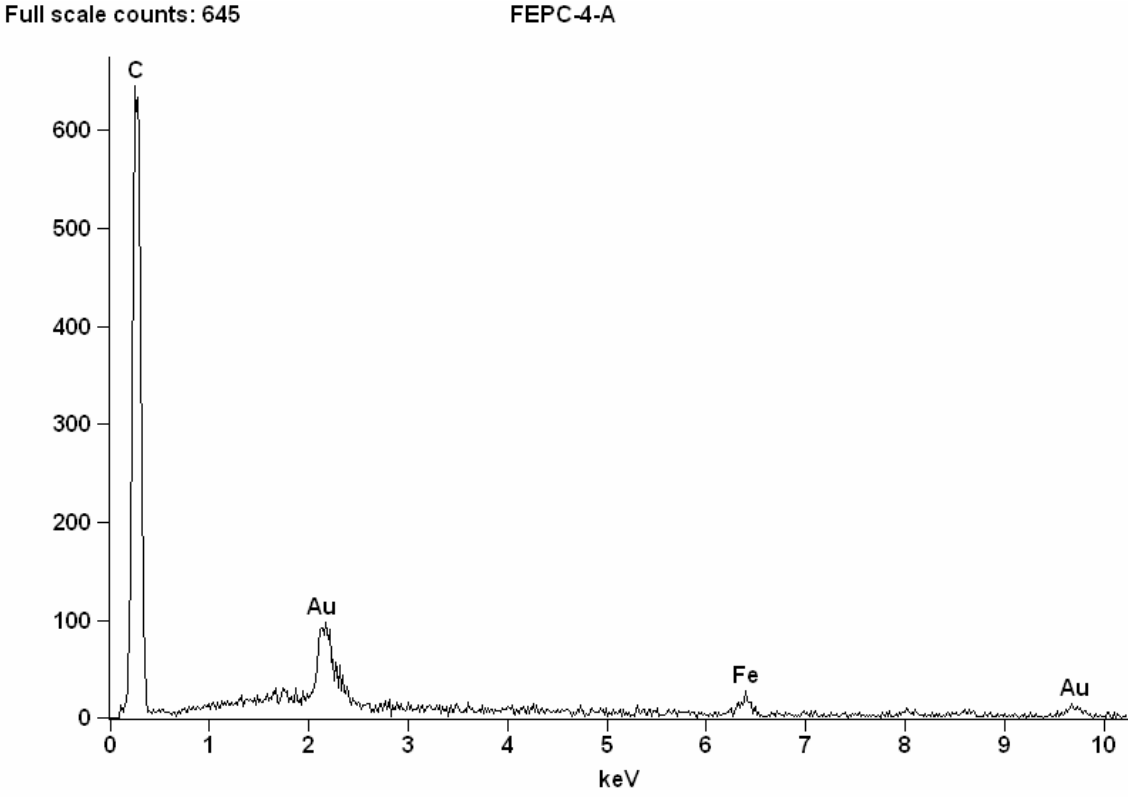

Figure 4.13 EDX spectra of the FePc impregnated on carbon black and pyrolyzed at 1000^{o}C

4.2.3. SEM Micrographs and EDX Spectra of Nickel Phthalocyanine

Similar analysis for NiPc/C was also performed by SEM and EDXS. In Figure 4.14, the SEM micrographs of the NiPc/C pyrolyzed at 1000^{o}C are given at 400 and 5000 times of magnifications. When the particle surface was analyzed in detail, a homogenous particle surface with a well porous structure is seen.

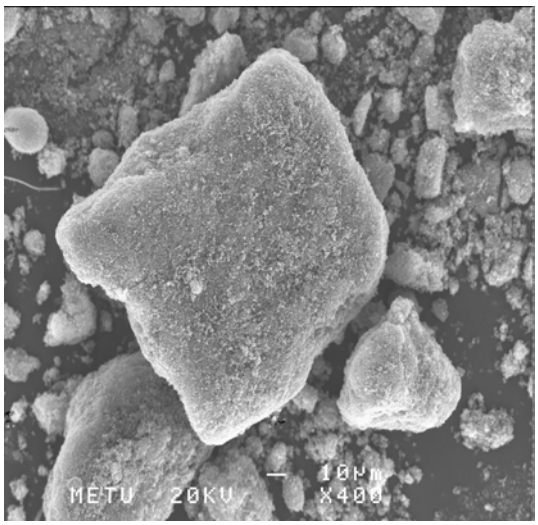

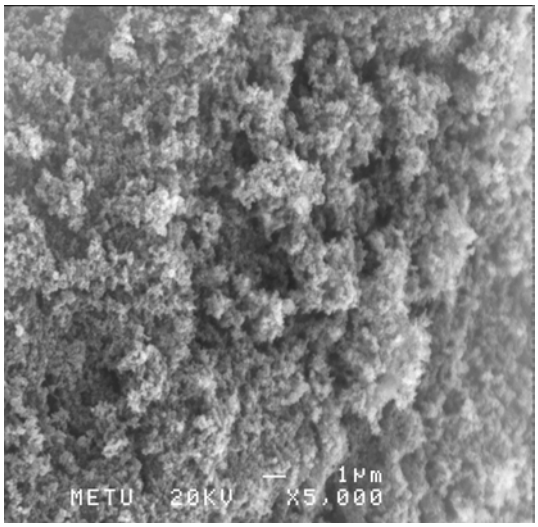

Figure 4.14 SEM micrographs of the NiPc impregnated on carbon black and pyrolyzed at 1000^{o}C

The EDX spectrum obtained for NiPc/C pyrolyzed at 1000^{o}C is given in Figure 4.15. Since the main part of the catalyst consists of carbon, the carbon peak observed was the highest peak which was a definitely expected result. As being in all of the cases, the gold peaks in the EDX spectra of the catalyst sample are due to the gold coating used during the specimen preparation step. The impregnated catalyst is reported to have nickel, which verifies the surface contains the impregnated NiPc.

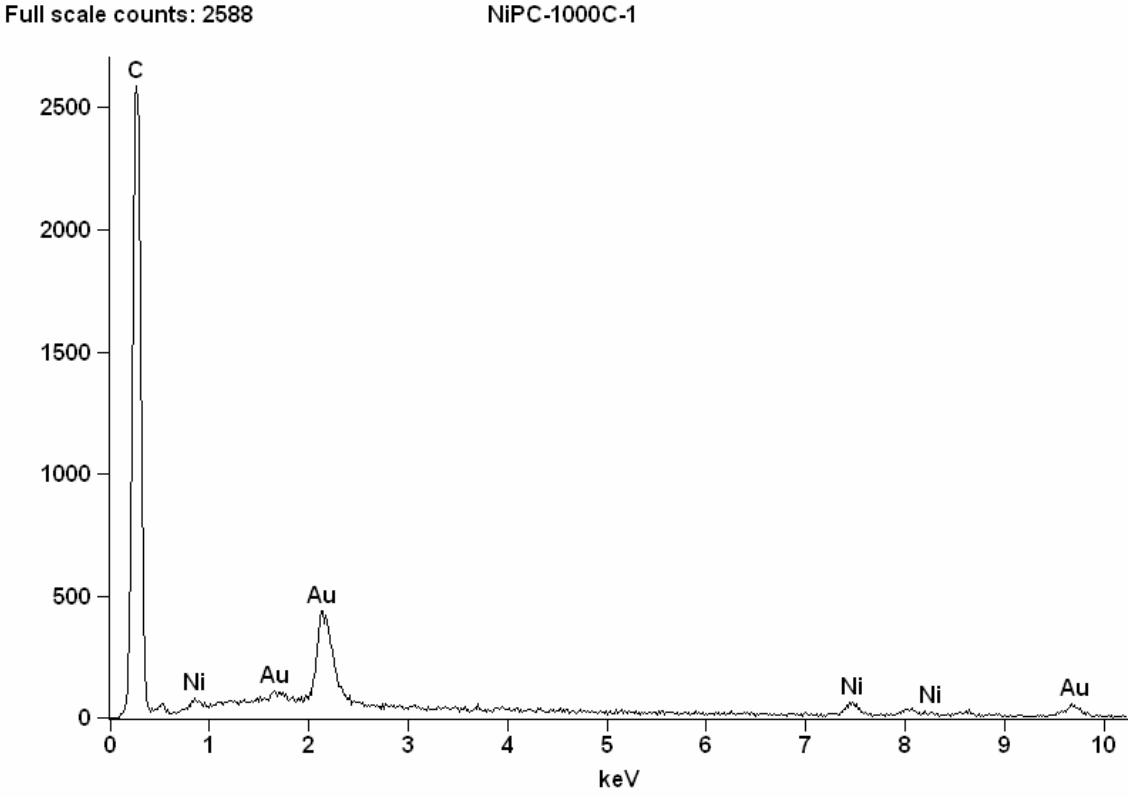

Figure 4.15 EDX spectra of the NiPc impregnated on carbon black and pyrolyzed at 1000^{o}C

4.3. Porosimetric Analysis of the Prepared Catalysts

The porosimetric data of the carbon black (Vulcan XC-72), cobalt phthalocyanine impregnated on carbon black either unpyrolyzed or pyrolyzed at 1000^{o}C and iron phthalocyanine impregnated on carbon black are summarized in Table 4.2. The BET surface area of the carbon black (Vulcan XC-72) which was used as catalyst support throughout the study was found as 180 m^2/g. The impregnation of the cobalt or iron phthalocyanines was caused to the decrease of the BET surface areas. The resulting BET surface areas for cobalt phthalocyanine impregnated on carbon black and iron phthalocyanine impregnated on carbon black were 81 and 86, respectively. The

pyrolysis of the cobalt phthalocyanine impregnated catalyst did not result an increase in the surface area. Contrarily, the BET surface area of the catalyst was slightly decreases from 81 m^2/g to 73 m^2/g. The micropore area of the carbon black catalyst support was found to be 29 m^2. However, the micropores existing on the carbon black support were disappeared during the impregnation process. Average pore volume and size increased when the phthalocyanines were impregnated on the carbon black. Average pore diameters are in the mesopore range defined by IUPAC as 20-500 Å.

Table 4.2 Porosimetric data of carbon black and some catalysts used in the study

	Vulcan XC-72	CoPc/C Tp=0°C	CoPc/C Tp=1000°C	FePc/C Tp=0°C
AREA				
BET Surface Area (m^2/g)	180	81	73	86
BJH cumulative adsorption surface area of pores between 17 and 3000 A diameter (m^2/g)	125	85	64	90
Micropore area (m^2/g)	29	0	10	0
VOLUME				
BJH cumulative adsorption pore volume of pores between 17 and 3000 Å diameter (cc/g)	0.25	0.22	0.15	0.22
Micropore volume (cc/g)	0.013	0	0.0040	0
PORE SIZE				
Average pore diameter (4V/A by BET) (Å)	55	109	81	101
BJH adsorption average pore diameter (Å)	80	106	91	98

The pore sizes are classified by IUPAC as macropore for pore size≥ 500 Å, mesopore for pore size is from 20 to 500 Å, supermicropore for pore size is from 7 to 20 Å, and ultramicropore for pore size≤7 Å (Lastoskie et.al., 1992) . The pore size distributions of carbon black support (Vulcan XC72) and CoPc impregnated on carbon black support are given in Figure 4.16. According to IUPAC classification, the carbon black used as a catalyst support in the study has mesoporous pores having mostly 20 Å and 40 Å sizes. It is also seen in the Figure 4.16 that the impregnation of cobalt phthalocyanine was destroyed the mesopores of the Vulcan XC72. However, the evolution of new mesopores of 400 Å pore size can be seen. An interesting pore evolution at 750 Å was observed which indicates the pore size was shifted to macropore range.

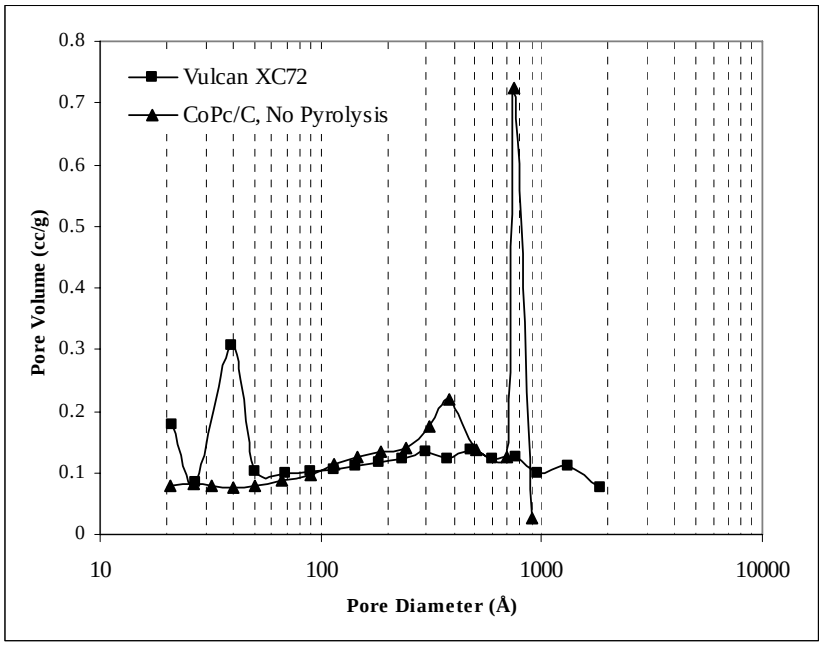

Figure 4.16 Comparison of pore size distributions of carbon support (Vulcan XC-72) and CoPc/C without pyrolysis

The pore size distribution of CoPc/C pyrolyzed at 1000^{o}C was compared with Vulcan XC72 in Figure 4.17. One may expect new pores to be formed when the CoPc material was decomposed. However, pyrolysis of the impregnated catalyst did not result evolution of micro or mesopores. Contrarily, the mesopores at 400 Å range and the macropores at 750 Å were disappeard. New macropores at 1000 Å range were formed.

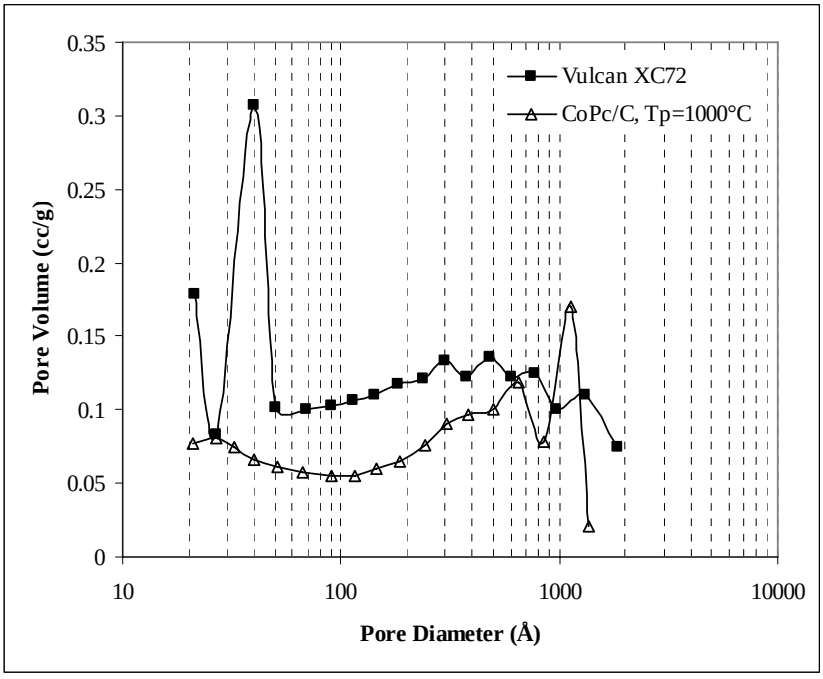

Figure 4.17 Comparison of pore size distributions of carbon support (Vulcan XC-72) and CoPc/C pyrolyzed at 1000^{o}C

The pore size distributions of FePc/C were compared with Vulcan XC72 in Figure 4.18. The behavior of CoPc impregnation was observed also in the case of the impregnation of the FePc. That is, the impregnation caused the mesopores of the Vulcan XC72 to be disappeard. Moreover, some new pores were obtained in the meso and macropore range.

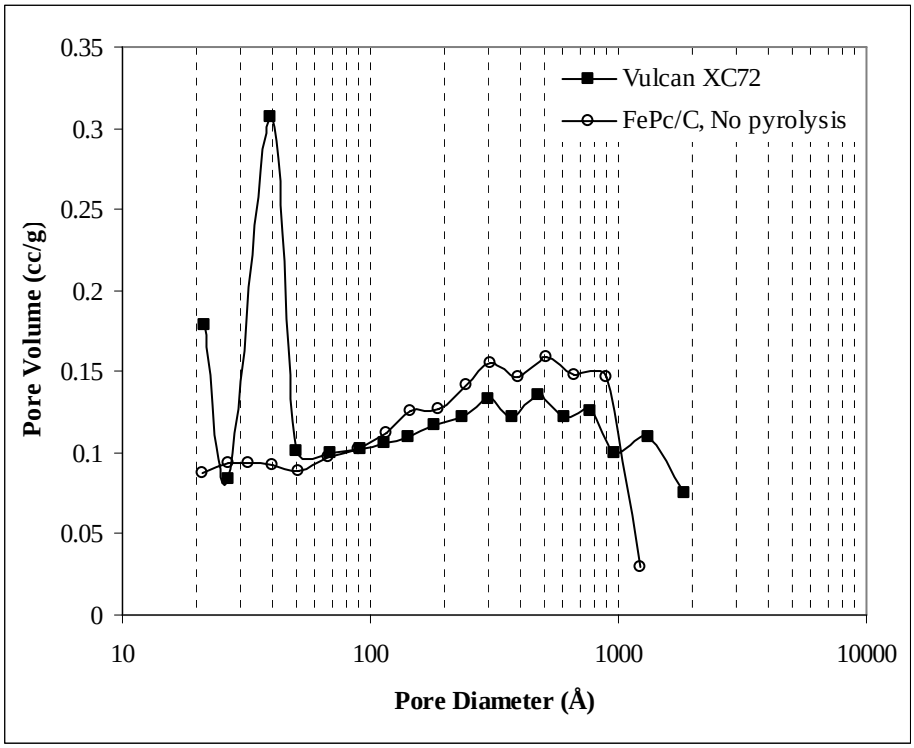

Figure 4.18 Comparison of pore size distributions of carbon support (Vulcan XC-72) and FePc/C without pyrolysis

The comparison of the pore size distributions of the CoPc/C unpyrolyzed and pyrolyzed at 1000^{o}C catalysts is given in Figure 4.19. It can be clearly seen that the pyrolysis does not improve the pore structure.

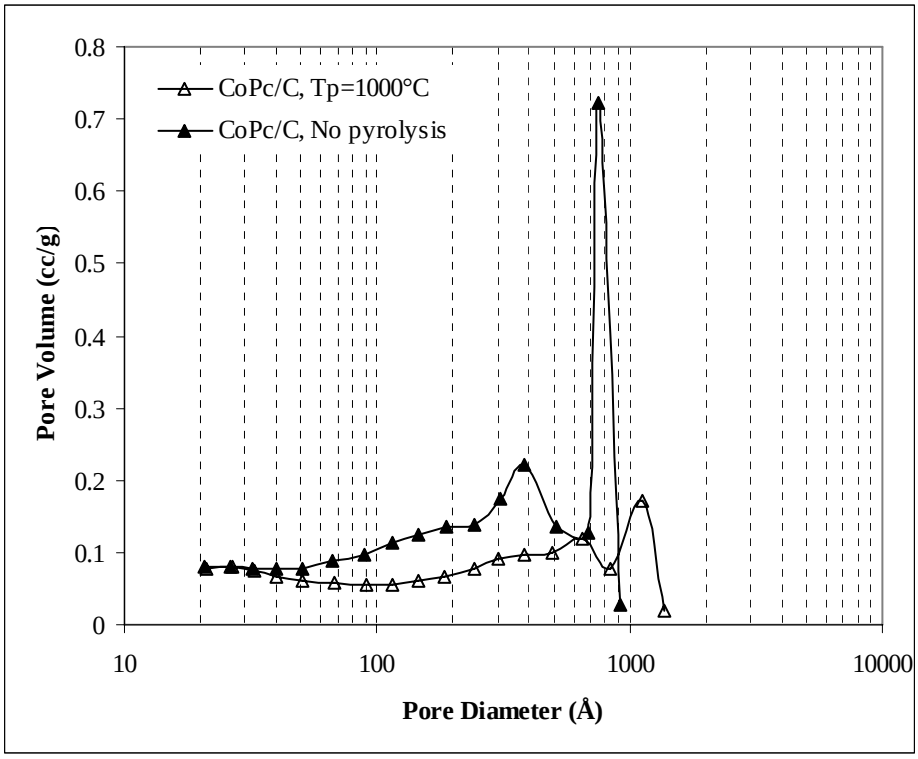

Figure 4.19 Comparison of pore size distributions of CoPc/C pyrolyzed at 1000^{o}C and CoPc/C without pyrolysis

The pore size distribution of unpyrolyzed FePc/C catalyst was compared with unpyrolyzed CoPc/C catalyst in Figure 4.20. Except the macropore observed for CoPc/C the pore size distributions of FePc/c and CoPc/C were very similar.

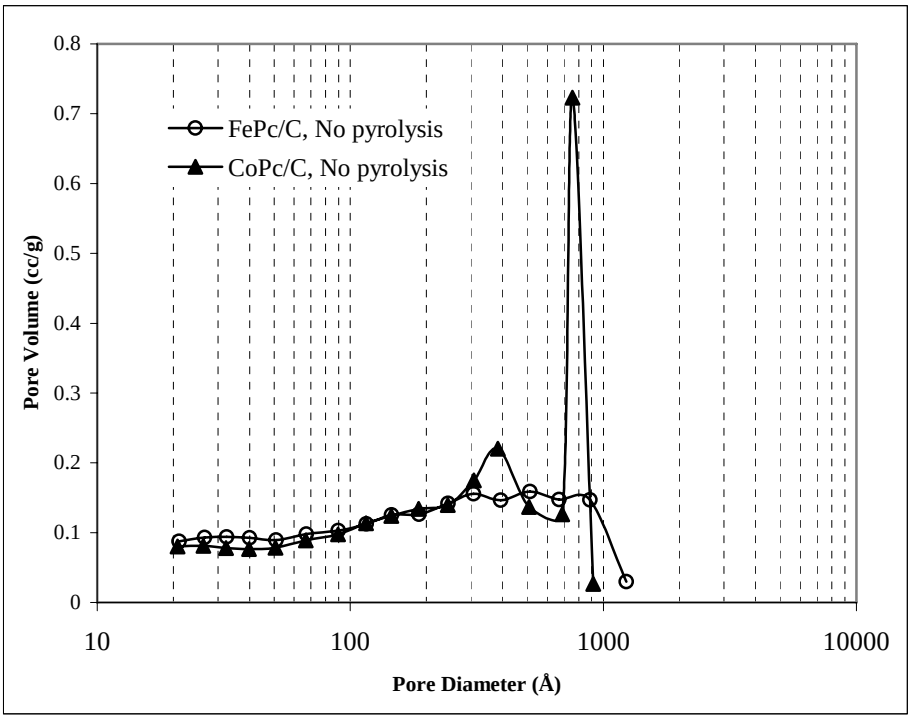

Figure 4.20 Comparison of pore size distributions of FePc/C and CoPc/C without pyrolysis

4.4. The Performance of the Fuel Cells Built with Metalo Phthalocyanine Cathode Catalysts

4.4.1. The Effect of Pyrolysis Temperature

Influence of the pyrolysis temperature on the performance of the PEM fuel cells with phthalocyanines was examined. In order to visualize the effect, the membrane electrode assemblies were prepared with three different CoPc and three different NiPc cathode catalysts. The resulting polarization curves which indicate the performance of the catalysts prepared with different pyrolysis temperatures are given in Figure 4.21 and Figure 4.22.

For the CoPc cathode catalysts the highest activity obtained at pyrolysis temperature of 1000°C. The performance improved with increasing pyrolysis temperatures. Figure 4.21 indicates that sole modification of the preparation of the cathode catalyst influences the overall performance of the PEM fuel cell. The performance improvement appears including OCV difference, activation polarization losses and ohmic polarization losses. When the catalysts were heat treated, higher open circuit voltage (OCV) such as 0.77V was obtained than the unpyrolyzed catalyst which exhibited an OCV of 0.6V.

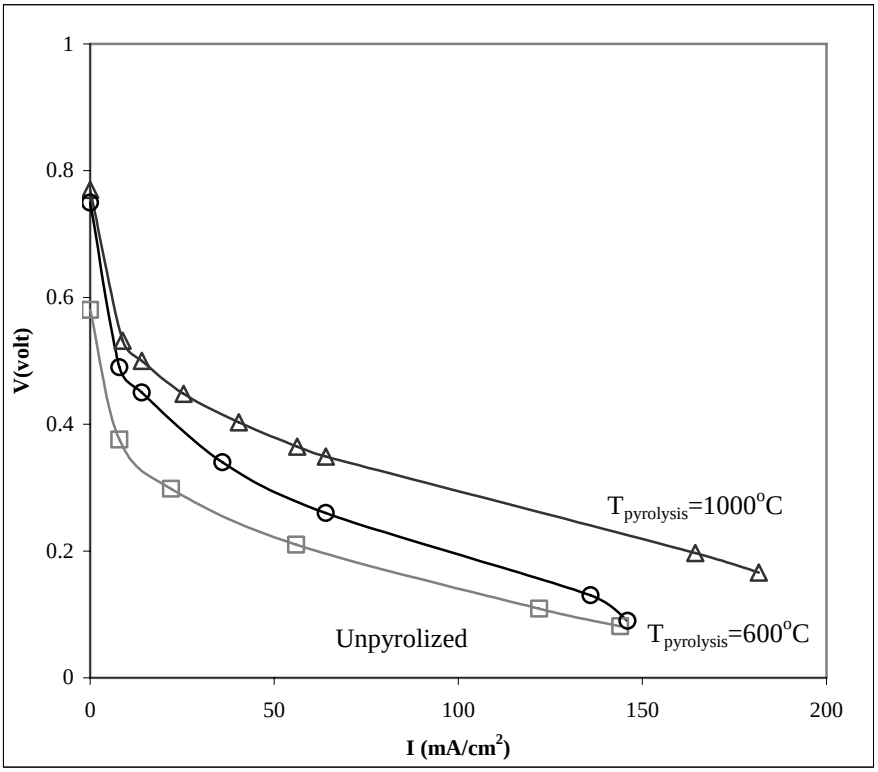

Figure 4.21 The effect of the pyrolysis temperature of cobalt phthalocyanine on the performance of the PEM fuel cell

The sudden decrease in the cell potential at lower current densities is due to activation polarization loss. Similar activation polarization losses were obtained for the cases having different pyrolysis temperatures. The ohmic polarization controls the performance at higher current densities. The smaller the slope of the polarization curve at higher current densities is the lower the ohmic polarization losses.

Similar trend was obtained for the NiPc catalysts as illustrated in Figure 4.22. However, the performances of the fuel cells prepared with NiPc cathode catalysts were very low. The sudden decrease on the activation losses region also indicates that a kinetic problem occurs in the fuel cell. It might be concluded that membrane electrode assemblies prepared with NiPc catalyst did not work.

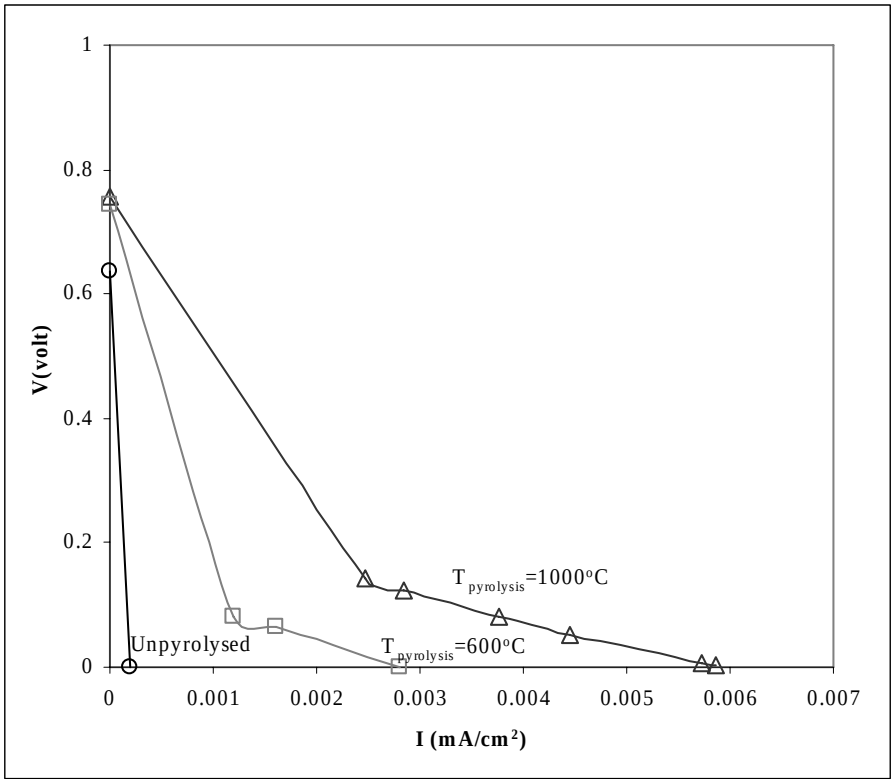

Figure 4.22 The effect of the pyrolysis temperature of nickel phthalocyanine on the performance of the PEM fuel cell

4.4.2. The Effect of the Catalyst Load

One may anticipate that increasing the metal content on a unit area should increase the performance of the fuel cell. To test this effect on the performance of PEM fuel cell, cobalt loading (in the CoPc/C form, pyrolyzed) of 0.14 and 0.28 mg Co/cm^2 was used. It was not possible to increase the cobalt loading more than 0.28 mg Co/cm^2 by using CoPc/C catalyst having 4% cobalt since the electrode thickness reached the physical limits of the electrode preparation technique. The effect of the Co loading on the performance of PEM fuel cell is illustrated in Figure 4.23. Open circuit voltages (OCV) were 0.77V in both loadings. The abrupt decrease of the cell voltage on the lower current densities indicates the existence of activation polarization losses. Namely, the kinetics of the system is sluggish. When the cobalt loading was increased to 0.28 mg/cm^2, the activation polarization loss decreased. In other words, the reaction rate is increased. At higher current densities the polarization curves of the both loadings were parallel which indicates that both membrane electrode assemblies are under the same effect of ohmic polarization losses. Shortly, the increase in the catalyst loading positively affected the reaction kinetics and increased the overall performance of the PEM fuel cell.

Since the electrode layer thickness reached its physical limits, further increase in the catalyst loading might be achieved by an increase in the catalyst amount on the carbon black.

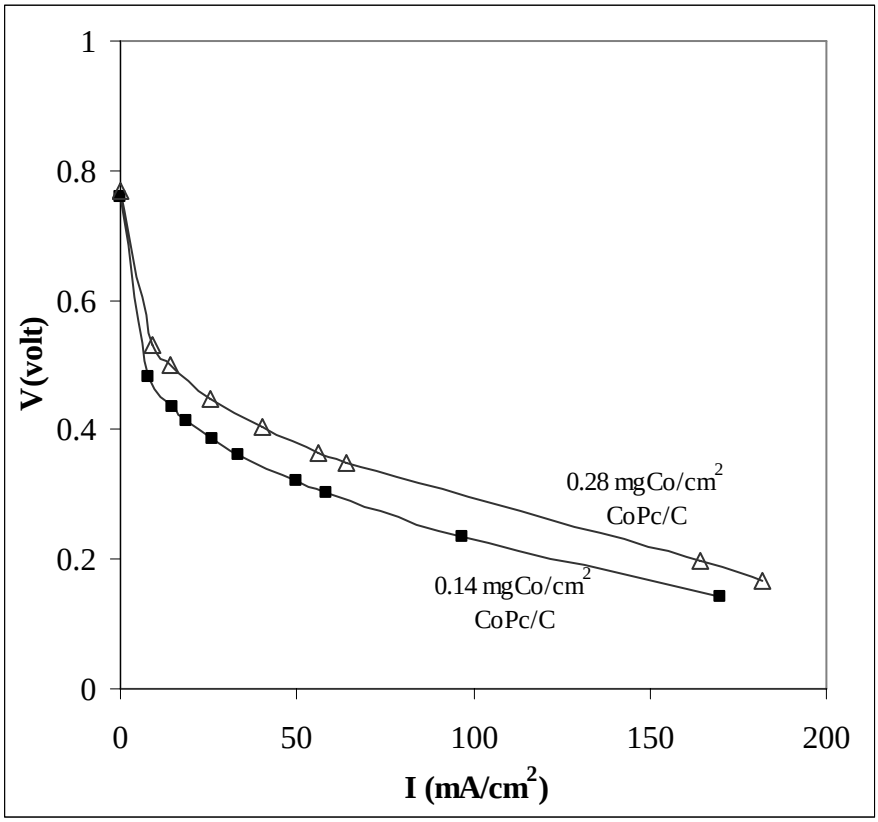

Figure 4.23 The effect of the Cobalt loading to the performance of the PEM fuel cell (Pyrolysis temperature is 1000°C)

4.4.3. The Effect of the Catalyst Content of the Carbon Black

The effect of the catalyst content of the carbon black on the performance of the PEM fuel cell was investigated by increasing the impregnation content of iron phthalocyanine on carbon black from 4% to 10%. The polarization curves were obtained by the performance analysis of the PEM fuel cells prepared with 4% Fe content and 10% Fe content. The effect of iron phthalocyanine content impregnated on the carbon black was illustrated in Figure 4.24. Increasing iron content of the carbon black, increased the activation polarization loss of the cell. Not only the activation polarization loss observed in the cell but also the ohmic polarization losses increased at higher current densities.

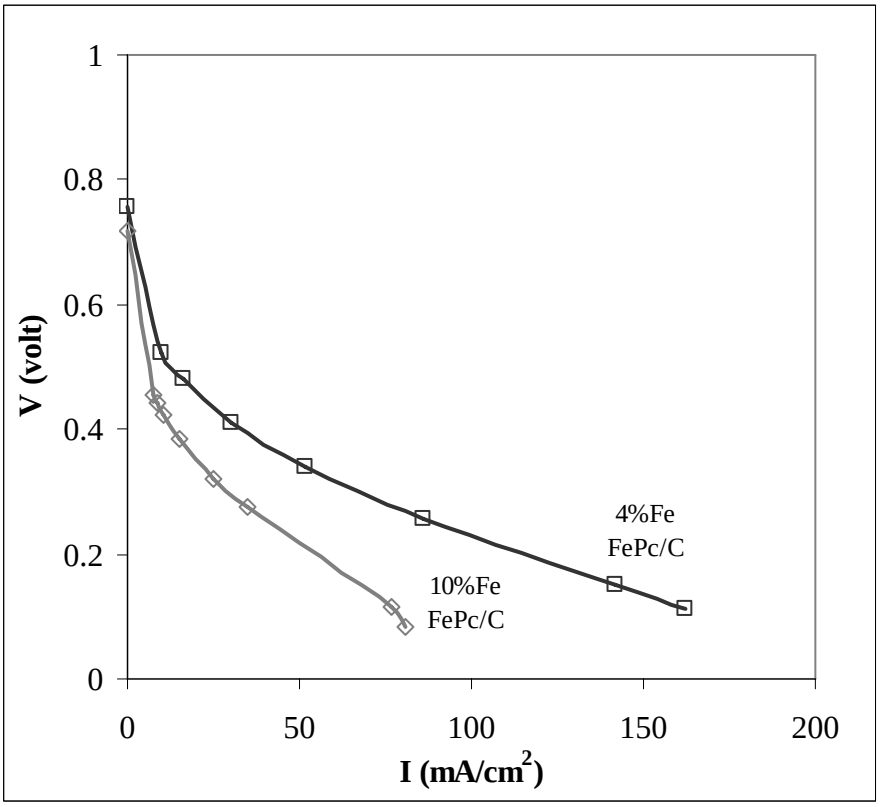

Figure 4.24 The effect of iron phthalocyanine content impregnated on the carbon black. (Pyrolysis temperature is 1000^{o}C)

Metalo phthalocyanines are macro cyclic molecules that have approximately MW of 570g/mol. Therefore, effective dispersion of the active sites inside the carbon black pores might not been maintained.

The result obtained is in the present study is compared with the results reported Faubert et al., (1998). They used iron tetraphenylporphrin as catalyst, that contained 2%, 4% and 6% Fe loadings on the carbon black After pyrolysis at 1000°C the resulting activity order was found as 4>2>6 wt%.

As for CoPc, the highest activity was obtained when 4% cobalt based initial loading was employed and pyrolyzed at 1000°C. Similarly, the highest catalytic activity for FePc was obtained when 4% iron based initial loading was used to prepare FePc/C and pyrolyzed

at 1000°C. However, the resulting performances were less than the one for the PEM fuel cell with cathode which was manufactured with 0.4 mg Pt/cm^2 loading catalysts having 20%Pt/C. In the case of a commercial Pt based membrane electrode assembly, the performance was found to be even higher. All these polarization curves are shown in Figure 4.25. Platinum based catalysts exhibited higher OCVs than phthalocyanine based catalysts. The highest OCV obtained for 0.4 mg Pt/cm^2 cathode was tested. However, the existence of the activation polarization loss caused a potential loss. Moreover, ohmic polarization losses significantly decreased the cell potential when the current increased. Commercial MEA exhibited the smallest activation and ohmic polarization losses.

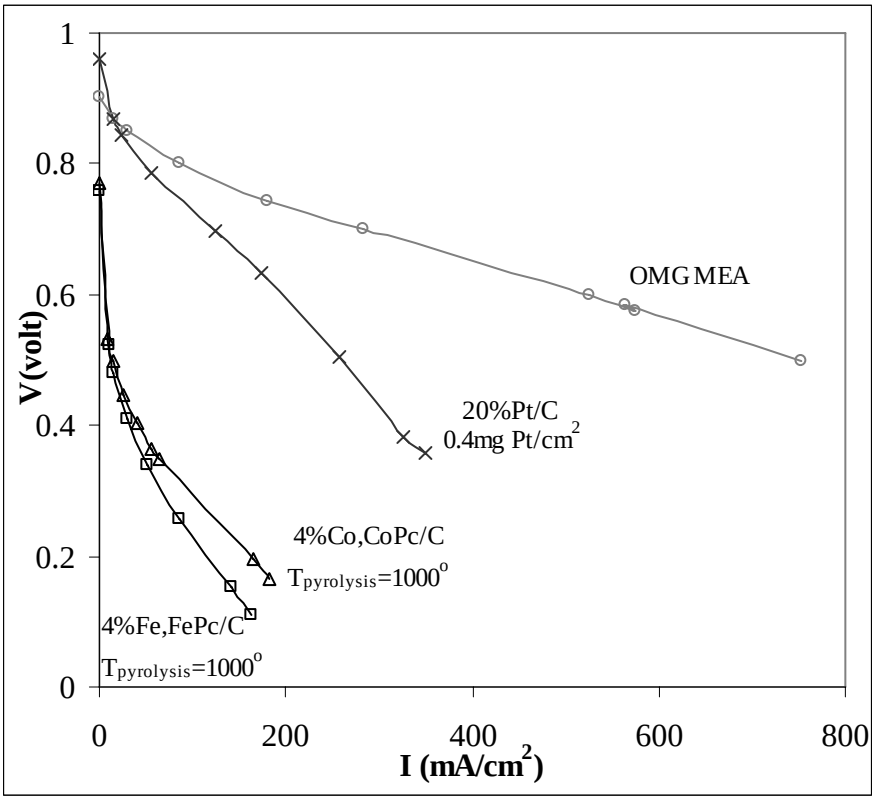

Figure 4.25 Comparison of the PEM fuel cell performances having cathodes with iron and cobalt phthalocyanine catalysts with the one containing platinum catalyst and commercial OMG MEA.

4.5. Discussion

In this study, the aim was to prepare and develop metalo phthalocyanine electrocatalysts for the cathode of the PEM fuel cell and to investigate the performance of the PEM fuel cells manufactured with these catalysts. Prior to this study, a test station was built and used for the fuel cell performance measurements for the development and optimization of the PEM fuel cells (Yazaydın, 2003). The test station was capable of obtaining polarization curves for an assembled test cell. However, there were some problems with the test station that the performances of the commercial MEAs were order of magnitude lower than the reported performances in the literature. Although, the aim of the study was to prepare, develop and test the metalo phthalocyanine catalysts, first step of the study was to develop a reliable test station which is capable of testing PEM fuel cells. In addition to this study, parallel work has been conducting on the development of the PEM fuel cells tolerant to CO and CO_2 by PhD. student Ayşe Bayrakçeken. Therefore, the test station had to be improved in a short time and the literature performances must have been reached.

The importance of the humidification was realized and the humidifying system was checked. It was understood that the gases passing through the humidifiers did not reach the fuel cell at the saturation level of the humidifier. The reason of low humidification at the test fuel cell was the unheated gas transfer hoses. Just simple insulation of the lines were not sufficient for the gases to keep its temperature to reach fuel cell and the humidity of the gases were lost in the hoses. In order to solve this problem, gas transfer hoses having active heating were built by using resistance wire and the temperature of this electric heater was controlled by a temperature controller.

The test system was not able to operate at high pressures (50 psi) and it was operating at ambient pressure. For that reason, the components like humidifiers, gas transfer lines, fittings were rebuilt from stainless steel material to be able to operate at high pressures. However, two back pressure regulators could no be purchased and the tests were carried out at ambient pressure.

The final and the most critical problem of the system was found to be the gasket of the PEM fuel cell, surprisingly. The older gasket used was made of Teflon and it has 600 micron thickness. The gasket was changed to 200 micron silicone material.

The improvements explained above were resulted the test station to capable of making measurements similar to literature values for the commercial MEAs. However, the MEAs manufactured by using the prepared metal phthalocyanine catalysts could not reach the MEAs manufactured with platinum catalysts. Metalo phthalocyanine compositions used in the present work are very dilute for impregnation. Also, the sizes of metalo phthalocyanines are quite long comparing with the size of the metal. Therefore, the development of a technology for preparing high loading of phthalocyanine catalysts might be increase the performance of the MEAs manufactured with phthalocyanines. Alternatively, in the future, new materials having metal-nitrogen bond in a carbon matrix with smaller size should be searched.

Metalo phthalocyanines prepared in the present work could be dissolved in concentrated sulfuric acid. During impregnation, SO_3^- was adsorbed on carbon black. Since the affinity of SO_3^- to the carbon black is very high, it was not possible to eliminate the adsorbed SO_3^- from the catalyst surface by successive washing. Sulfur peak appeared in the EDX spectra of the unpyrolyzed catalyst. It was good to observe that sulfur could be eliminated by pyrolysis of the catalyst. It should be emphasized that sulfur is a poison for nickel. Me-S might form for the other metals also. Therefore, unpyrolyzed catalysts might perform lower activity due to the adsorbed SO_3^- on the carbon black.

CHAPTER 5

CONCLUSIONS AND RECOMMENDATIONS

The importance of the sustainable and renewable energy sources have been understood in the past few decades. It is inevitable that the lack of the fossil fuels will require an energy revolution. Most of the scientists, technologists and industrial people have accepted that hydrogen will be the energy carrier of the future. Once the hydrogen is obtained from renewable primary energy sources, such as solar and wind energy, the utilization of the hydrogen can be achieved in order to produce useful energy for the specific needs of the people.

Fuel cells were accepted by the authorities to be the energy converters of the hydrogen energy. Fuel cells are highly efficient devices that convert the chemical energy of the hydrogen to directly electricity and heat. The main problem of the fuel cells to be commercialized is the cost of the materials used and the life of the membrane electrode assemblies which is the heart of a PEM fuel cell system. One of the key components which increases the cost and does not have long life is the catalyst used at the anodes and the cathodes of the membrane electrode assemblies. Platinum adsorbed on the carbon black support are the catalysts currently used in the PEM fuel cells.

The aim of this study was to prepare some metalo phthalocyanine catalysts for the cathode side of the PEM fuel cells where the oxygen reduction reaction occurs and to test the performance of the PEM fuel cells built with the prepared metalo phthalocyanine based catalysts.

The phthalocyanines of the cobalt, iron and nickel were synthesized by phthalic anhydride-urea process. The characterization of the synthesized cobalt phthalocyanine was done by infrared spectrometry and X-ray diffractometry. Infrared spectrometry was used for the characterization of the iron and nickel phthalocyanines. The results of the analyses were proved that the materials synthesized were indeed the phthalocyanines of cobalt, iron and nickel.

The fuel cell cathode catalysts were prepared by impregnating the 4% cobalt, 4 or 10% iron or 4% nickel phthalocyanines on to the carbon black support. In order to increase the activity and the stability of these catalysts, heat treatment (pyrolysis) was done at 600 or 1000^{o}C under nitrogen atmosphere. The characterization of the prepared catalysts was done by scanning electron microscopy (SEM) and energy dispersive X-ray spectroscopy (EDXS) analyses. SEM micrographs indicated that the porous structure of the carbon black was preserved during the impregnation and pyrolysis steps. There is no evidence to prove that phthalocyanines were dispersed evenly on the surface of the carbon black. For the unpyrolyzed CoPc/C, sulfur atom was detected by the EDXS analysis. The reason of the existence of the sulfur atom on the carbon black surface is supposed to be due to the sulfuric acid used in the impregnation process. When the catalyst samples were pyrolyzed, the sulfur atom disappeared. The reason of this must be the thermal decomposition of the sulfuric acid since it has a thermal decomposition temperature of 340^{o}C.

The membrane electrode assemblies were prepared by using the platinum catalyst for the anodes and the presently prepared catalysts for the cathode. The electrodes were prepared on the to the gas diffusion layers by the spraying technique. The platinum load for the anode was kept constant as 0.4 mg/cm^{2}. The cathode electrodes were prepared with 0.3 mg metal (Co,Fe or Ni) loading basis. In addition to the CoPc/C having 0.3 mg Co/cm^{2} metal loading, , 0.14mg Co/cm^{2} loading electrode was also prepared for the CoPc/C pyrolyzed at 1000^{o}C catalyst in order to visualize the effect of the loading on the overall performance of the fuel cell.

Experiments indicated that cobalt phthalocyanine based cathode catalysts are more active than iron phthalocyanine based catalysts. The increased pyrolysis temperature showed a positive effect on the performance of the fuel cell prepared with cobalt phthalocyanine catalytic cathodes. The highest activity was obtained when the pyrolysis temperature was 1000°C. Whereas, unpyrolyzed cobalt phthalocyanine impregnated on carbon black exhibited low performance. Increasing the impregnated catalyst amount did not result an increase in the performance. Contrarily, the performance of the iron phthalocyanine with 10% loading on the carbon black gave lower performance. Nickel phthalocyanine based catalysts, either unpyrolyzed or pyloyzed at 600 or 1000^{o}C did not exhibit a catalytic effect. That is the fuel cells prepared with these catalysts did not work.

The highest performance was observed with the commercial membrane electrode assembly which is known to have platinum based catalysts on the anode and cathode electrodes. The power densities obtained from commercial MEA was 0.36W/cm^2 and 0.40W/cm^2 for 0.6 and 0.5 volts respectively. Whereas, the power density obtained from the MEA manufactured at the laboratory with 0.4 mg Pt/cm^2 both on the anode and cathode was 0.13W/cm^2 0.18 W/cm^2 at 0.6V and 0.5V, respectively. For the phthalocyanine cathodic MEAs, the highest power reached was 0.04W/cm^2 which was obtained from the MEA prepared with the CoPc/C with a loading of 0.28mg Co/cm^2.

The performance of the MEA produced in our laboratory by using Pt/C catalyst on both anode and cathode sides is about half of the commercially available MEA. If this performance difference is not simply because of the platinum load of the electrodes, an improvement for the preparation technique of the MEAs must be developed. The Nafion content of the catalyst ink might be optimized in order to increase the ionic conductivity between the catalyst particles and the membrane. The application of the catalyst ink to the membrane surface would also affect the performance. That is, either the catalyst is first applied to the membrane or GDL in order to form electrode layer might change the performance. Another important parameter while producing the MEA is the compressive force applied to the MEA during the production period. The optimization of this pressing pressure might result better performances.

The catalytic effects of some of the phthalocyanines have been observed throughout the study. However, the performances of the fuel cells built with phthalocyanine based cathodic catalysts are not compatible with the platinum catalysts. Since the different kinds of phthalocyanines of the metals exhibit different performances, more metalo phthalocyanine compounds should be tried. Moreover, the metalo phthalocyanine contents impregnated on the carbon black must be increased. The importance of increasing the metal content of the carbon black is that when the metal content is increased, the amount of the MePc/C applied to the surface is decreased. Therefore, the electrode layer thickness is reduced which results in the effective use of the catalyst and the easy transport of the protons to the Nafion membrane.

REFERENCES

1. Achar B.N., Lokesh K.S., Fohlen G.M., Mohan Kumar T.M., “Characterization of cobalt phthalocyanine sheet polymer by gas chromatography mass spectrometry on its pyrolysis products”, Reactive & Functional Polymers 63, 63–69, 2005.

2. Bevers D., Wagner N., Bradke M.Von, “Innovative production procedure for low cost PEFC electrodes and electrode/membrane structures”, Int. J. Hydrogen Energy, 23, No.1, 57-63, 1998.

3. Cooper, S.J. , in Proceedings of the Second International Symposium on New Materials for Fuel Cell and Modern Battery Systems, Montreal, July 6-10, 1997, p 286.

4. Faubert G., Cote R., Guay D., Dodelet J.P., Denes G., Bertrand P., “Iron catalysts prepared by high-temperature pyrolysis of tetraphenylporphyrins adsorbed on carbon black for oxygen reduction in polymer electrolyte fuel cells” Electrochimica Acta 43 (3-4): 341-353, 1998.

5. Fuel Cell Handbook, U.S. Department of Energy, Office of Fossil Energy, National Energy Technology Laboratory. 5th Ed., 2000.

6. Gamburzev S., Petrov K., Appleby A.J., “High Active Oxygen Reduction Electrocatalyst for Alkaline Fuel Cells and Metal-Air Batteries”, Abstract 353, Proceedings ofthe 200th ECS Meeting, 2001.

7. Gojkovic S.L., Gupta S., Savinell R.F., ” Heat-treated iron(III) tetramethoxyphenyl porphyrin chloride supported on high-area carbon as an electrocatalyst for oxygen reduction - Part II. Kinetics of oxygen reduction”, J. Electroanal. Chem., 462 (1): 63-72, 1999.

8. Hoogers G., “Fuel Cell Technology Handbook”, CRC Press, USA, (2002).

9. Jahnke H., Schönborg M., and Zimmermann G., Top. Curr. Chem., 61, 133, 1979.

10. Jang R.Z., Chu D.,” Remarkably active catalysts for the electroreduction of O_2 to H_2O for use in an acidic electrolyte containing concentrated methanol”, J. Electrochem. Soc. 147 (12), 4605-4609, 2000.

11. Jung K.S., Kwon J.H., Son S.M., Shin J.S., Lee G.D., Park S.S., “Characteristics of the copper phthalocyanines synthesized at various conditions under the classical and microwave processes”, Synthetic Metals, 141 (3): 259-264, 2004.

12. Kalvelage H., Mecklenburg A., Kunz U., Hoffmann U., “Electrochemical Reduction of Oxygen at Pyrolyzed Iron and Cobalt N4-Chelates on Carbon Black Supports”, Chem. Eng. Technol., 23, 803-807, 2000.

13. Kiefer J., Brack H.P., Huslage J., Büchi F.N., Tsakada A., Geiger F., and Schere G.G., “Radiation grafting: a versatile membrane preparation tool for fuel cell applications“ Proceedings of the European Fuel Cell Forum Portable Fuel Cells Conference, Lucerne, 227-235, 1999.

14. Kirk Othmer Encyclopedia of Chemical Technology, 4th Ed., John-Wiley and Sons Inc., N.Y., 1992.

15. Lalande G., Cote R., Tamizhmani G., Guay D., Dodolet J.P., Dignard-Bailey L., Weng L. T., Bertrand P., “Physical, Chemical and Electrochemical Characterization

of Heat-Treated Tetracarboxylic Cobalt phthalocyanine Adsorbed on Carbon Black as Electrocatalyst for Oxygen Reduction in Polymer Electrolyte Fuel Cells", Electrochemica Acta, 40: 2635-2646, (1995).

16. Lalande G., Faubert G., Cote R., Guay D., Dodolet J.P., Weng L.T., Bertrand P., " Catalytic Activity and Stability of Heat-Treated Iron Phthalocyanines for the Electroreduction of Oxygen in Polymer Electrolyte Fuel Cells", Journal of Power Sources, 61: 227-237, (1996).

17. Larminie, J., Dicks, A., "Fuel Cell Systems Explained", 2nd ed., John Wiley and Sons, London, 2003.

18. Lastoskie C., Gubbins K.E., Quirke N., "Pore Size Distribution Analysis of Microporous Carbons: A Density Functional Theory Approach", J. Phys. Chem., 97, 4786-4796, 1993.

19. Lefévre M., Dodelet J. P., Bertrand P., "O_2 Reduction in PEM Fuel Cells: Activity and Active Site Structural Information for Catalysts Obtained by the Pyrolysis at High Temperature of Fe Precursors", J. Phys. Chem. B,104, 11238-11247, 2000.

20. Oker L., MSc. Thesis in Chemistry Department, Middle East Technical University, Ankara, Turkey, 1985.

21. Passalacqua E . , Lufrano F . , Squadrito G ., Patti A ., Giorgi L ., "Nafion content in the catalyst layer of polymer electrolyte fuel cells : effects on structure and performance", Electrochimica Acta ,46 , 799-805, (2001).

22. Powder Diffraction File, Org. Phases Search Manual by Int. Center for Diffraction Data, 1989.

23. Qi Z., Kaufman A., “Enhancement of PEM fuel cell performance by steaming or boiling the electrode”, Journal of Power Sources, 109, 227-229, (2002).

24. R. P. Linstead, Br. Assoc. Adv. Sci. Rep. 1933, 465.

25. Sakamoto K., Ohno E., “Synthesis of cobalt phthalocyanine derivatives and their cyclic voltammograms”, Dyes and Pigments, 35 (4): 375-386, 1997.

26. Sasikumar G., Ihm J.W., Ryu H., “Dependence of optimum Nafion content in catalyst layer on platinum loading”, Journal of Power Sources 132, 11–17, 2004.

27. Segawa T., Maruyama K., Ninomiya T., Suyama M., “Process for Producing a Metal Phthalocyanine and/or Its Derivative”, United States Patent Office, 4906747, 1990.

28. Song J.M., Cha S.Y., Lee W.M., “ Optimal composition of polymer electrolyte fuel cell electrodes determined by the AC impedance method”, Journal of Power Sources, 94, 78-84, 2001.

29. Tokumitsu, K., Wainright, J.S., and Savinell R.F., “Electrochemical Properties of Pt/Carbon Ink Electrodes for Direct Methanol Polymer Electrolyte Fuel Cells”, Journal of New Materials for Electrochemical Systems, 2, 171-178, 1999.

30. Uchida, M., Aoyama, Y., Eda, N., Ogawa, M., “Solid polymer type fuel cell and method for manufacturing the same”, J Power Sources, 63, (2): 285, December 1996.

31. Ullmann ., “Ullmann’s Encyclopedia of Industrial Chemistry”, 6th Ed., USA, 2002.

32. Van Veen J.A.R., Visser C., “Oxygen Reduction on Monomeric Transition Metal Phthalocyanines in Acid Electrolyte”, Electrochimica Acta, 24, 921-928, 1979.

33. Wang H., Coté R., Faubert G., Guay D., and Dodolet J.P., “Effect of the Pre-Treatment of Carbon Black Supports on the Activity of Fe-Based Electrocatalysts for the Reduction of Oxygen”, J. Phys. Chem. B, 103, 2042-2049, 1999.

34. Wang L., Husar A., Zhou T., Liu H., “A parametric study of PEM fuel cell performances”, International Journal of Hydrogen Energy, 28, 1263–1272, 2003.
35. Yazaydın A.Ö., Eroğlu İ., Türker L., “Scanning Electron Microscopic Studies of Porous Carbon Electrodes Used In Alkaline Fuel Cells”, Chem Eng. Comm., 190, 976-985, 2003.

36. Yazaydın, A.Ö., MSc. Thesis in Chemical Engineering, Middle East Technical University, Ankara, Turkey., 2003.

APPENDIX A

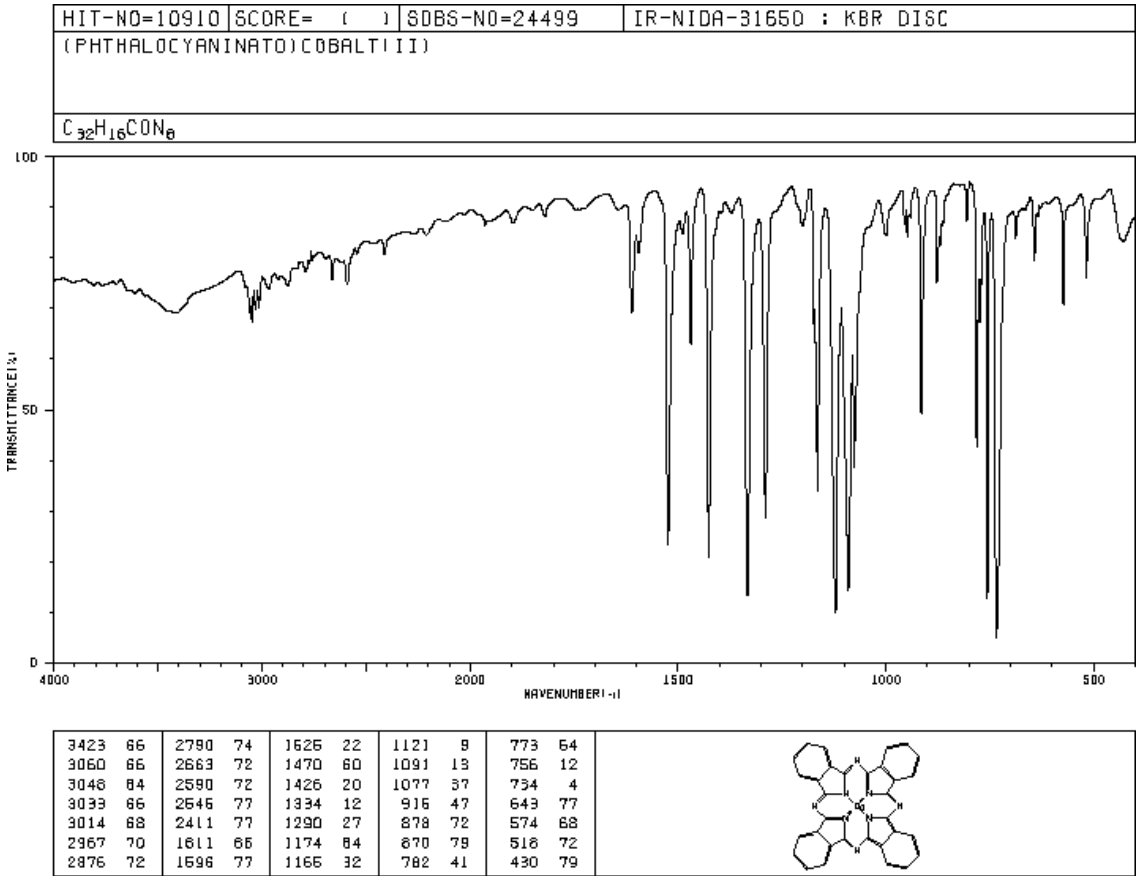

Figure A.1 The infrared spectrum of cobalt phthalocyanine in KBr pellet

(Ref: http://www.aist.go.jp/RIODB/SDBS/cgibin/cre_frame_disp.cgi?sdbsno=24499)

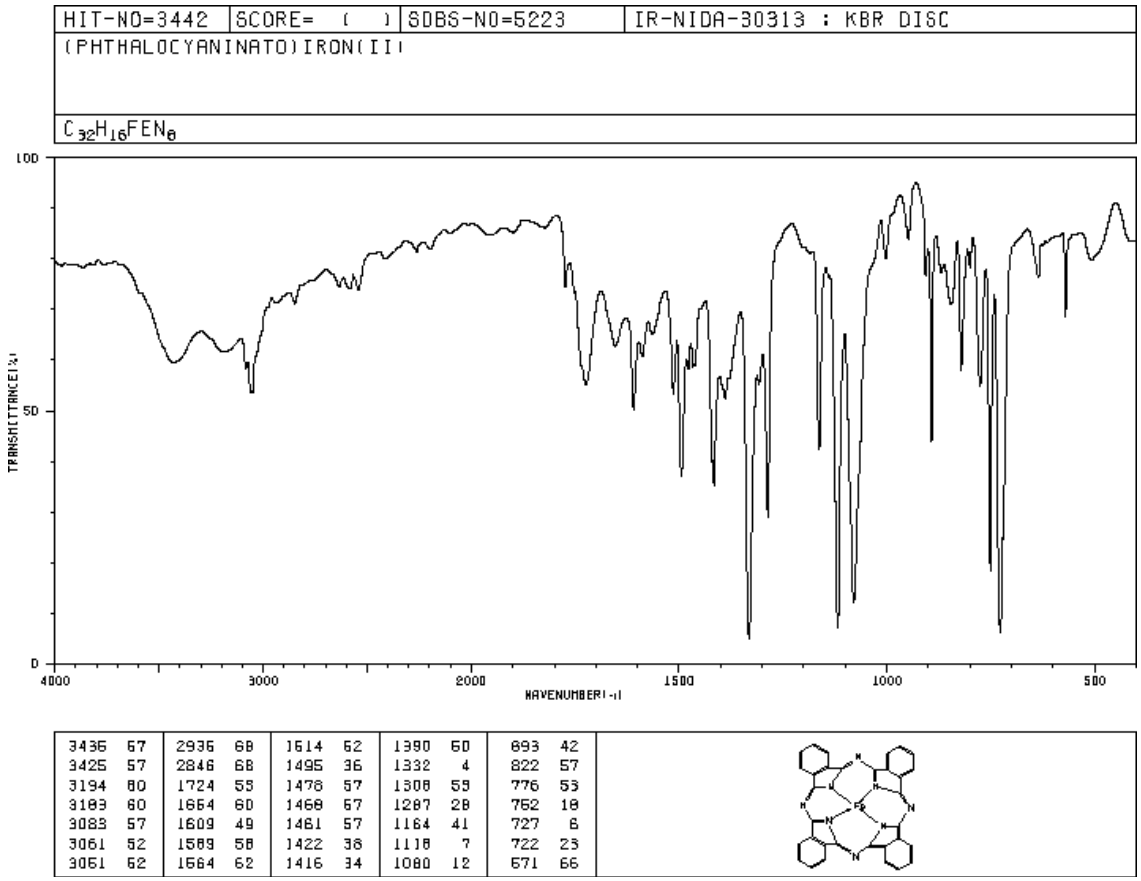

Figure A.2 The infrared spectrum of iron phthalocyanine in KBr pellet

(Ref: http://www.aist.go.jp/RIODB/SDBS/cgibin/cre_frame_disp.cgi?sdbsno=5223)

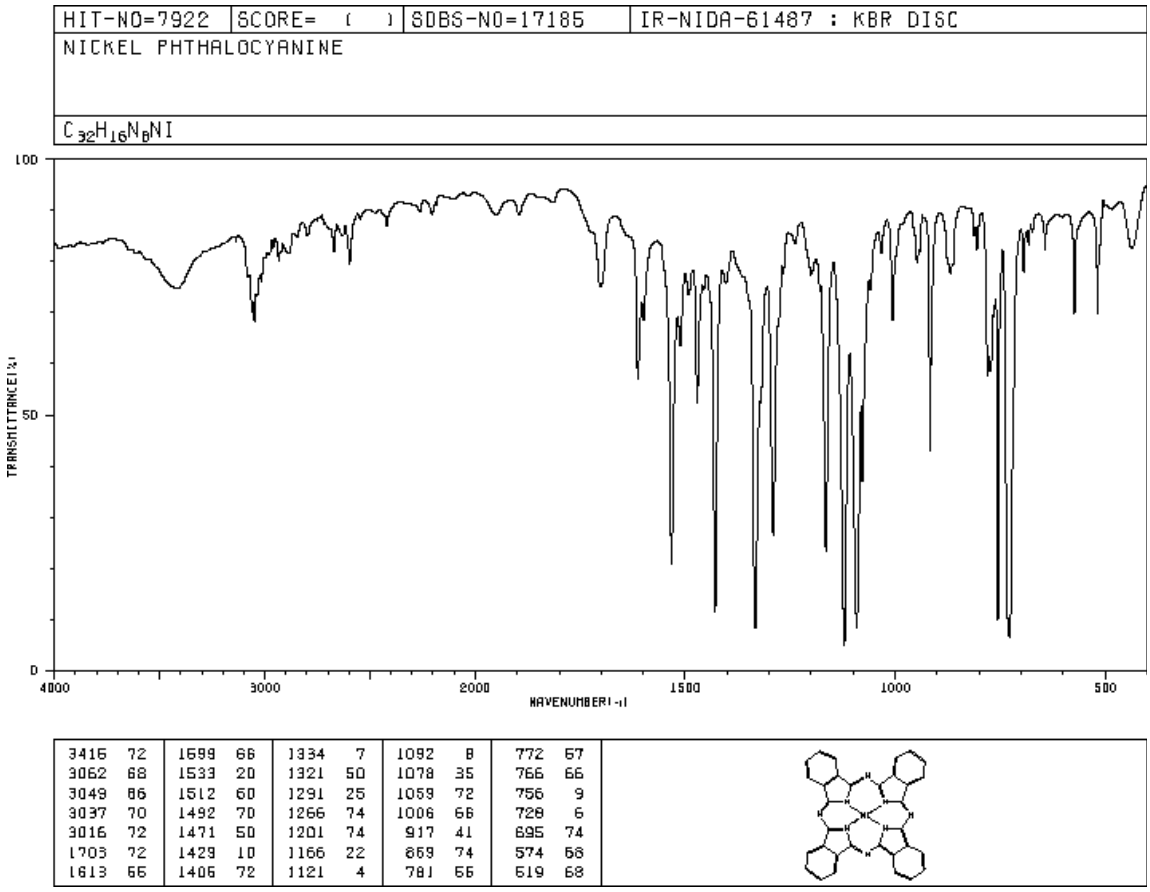

Figure A.3 The infrared spectrum of nickel phthalocyanine in KBr pellet

(Ref: http://www.aist.go.jp/RIODB/SDBS/cgibin/cre_frame_disp.cgi?sdbsno=17185)

APPENDIX B

```
Private Sub cmdExit_Click()
    frmRun.Hide
    frmDevSel.Show
    frmDevSel.cmdExit.SetFocus
End Sub

Private Sub cmdRead_Click()
    Dim tt As Long
    Dim Voltage As Single

    tmrRead.Enabled = True
    Timer2.Enabled = True
    Timer1.Enabled = True

    AiVolIn.chan = lpAIConfig.DasChan
    AiVolIn.gain = lpAIConfig.DasGain
    AiVolIn.TrigMode = AiCtrMode
    AiVolIn.Voltage = DRV_GetAddress(Voltage)
    shapLed.FillColor = QBColor(12)

    ErrCde = DRV_AIVoltageIn(DeviceHandle, AiVolIn)
    If (ErrCde <> 0) Then
      DRV_GetErrorMessage ErrCde, szErrMsg
      Response = MsgBox(szErrMsg, vbOKOnly, "Error!!")
```

```
      Exit Sub
    End If
    UpDateValue (Voltage)
End Sub

Private Sub cmdRead_MouseDown(Button As Integer, Shift As Integer, X As Single, y
As Single)
    shapLed.FillColor = QBColor(12)
End Sub

Private Sub Form_Load()
  Timer2_Timer
  Timer1_Timer
  Timer1.Interval = 250
  txtVoltRead_Click
  tmrRead_Timer
  hscrlFreq_Change

End Sub

Private Sub Form_Unload(Cancel As Integer)
    frmDevSel.Show
End Sub

Private Sub hscrlFreq_Change()
    If hscrlFreq.value = 0 Then
        tmrRead.Interval = 0
        Timer2.Interval = True
    Else
        tmrRead.Interval = 60000 / hscrlFreq.value
        Timer2.Interval = 60000 / hscrlFreq.value
```

```
    End If

    txtSample.Text = Format((hscrlFreq.value), "###0")

    tmrRead.Enabled = True
    tmrLed.Enabled = True
    Timer2.Enabled = True
    Timer1.Enabled = True
End Sub

Private Sub ReStart_Click()
    tmrRead.Enabled = True
    tmrLed.Enabled = True
    Timer2.Enabled = True
    Timer1.Enabled = True
End Sub

Private Sub stop_Click()
    tmrRead.Enabled = False
    Timer2.Enabled = False
    tmrLed.Enabled = False
End Sub

Private Sub tmrLed_Timer()
    shapLed.FillColor = QBColor(8)
End Sub

Private Sub Timer1_Timer()
  Dim Voltage As Single

  AiVolIn.chan = lpAIConfig.DasChan
```

```
  AiVolIn.gain = lpAIConfig.DasGain
  AiVolIn.TrigMode = AiCtrMode
  AiVolIn.Voltage = DRV_GetAddress(Voltage)
  ErrCde = DRV_AIVoltageIn(DeviceHandle, AiVolIn)
  If (ErrCde <> 0) Then
    DRV_GetErrorMessage ErrCde, szErrMsg
    Response = MsgBox(szErrMsg, vbOKOnly, "Error!!")
    Exit Sub
  End If
  UpDateValue (Voltage)
End Sub

Private Sub tmrRead_Timer()
  Dim Voltage As Single
  Static counter As Integer
  Dim Voltstore(10000) As Single
  counter = counter + 1
  shapLed.FillColor = QBColor(12)
  AiVolIn.chan = lpAIConfig.DasChan
  AiVolIn.gain = lpAIConfig.DasGain
  AiVolIn.TrigMode = AiCtrMode
  AiVolIn.Voltage = DRV_GetAddress(Voltage)
  ErrCde = DRV_AIVoltageIn(DeviceHandle, AiVolIn)
  If (ErrCde <> 0) Then
    DRV_GetErrorMessage ErrCde, szErrMsg
    Response = MsgBox(szErrMsg, vbOKOnly, "Error!!")
    Exit Sub
  End If
  Voltstore(counter) = Voltage
  voltval.AddItem Format(Voltstore(counter), "###0.0000")
  measno.Text = counter
```

```
End Sub
Private Sub UpDateValue(fValue As Single)
    ' Since the output box is too small to display all the digits
    ' of the input voltage, so it must use to format to get better
    ' display.
    txtVoltRead.Text = Format(fValue, "###0.000")
End Sub

Private Sub txtVoltRead_Click()
  tmrRead.Enabled = True
  tmrLed.Enabled = True
  Timer1.Enabled = True
End Sub

Private Sub Timer2_Timer()
    Dim currentTime As Date
    Static counter As Integer
    Dim Timestore(10000) As Single
    counter = counter + 1
    currentTime = Time
    Timestore(counter) = Time
    Timenow.Text = Format(currentTime, "ttttt")
    timebox.AddItem Format(Timestore(counter), "ttttt")
End Sub

Private Sub Voltshow(rValue As Single)
    VoltageArray.Text = Format(rValue, "###0.000")
End Sub

Private Sub Export_Click()
Dim xlApp As Excel.Application
```

```
Dim xlSh As Excel.Worksheet
Dim i As Long
Dim y As Long

Set xlApp = New Excel.Application

xlApp.Visible = True
xlApp.Workbooks.Add
Set xlSh = xlApp.Workbooks(1).Worksheets(1)

For i = 1 To timebox.ListCount
   xlSh.Cells(i, 1).value = timebox.List(i - 1)

Next

      For y = 1 To voltval.ListCount
        xlSh.Cells(y, 2).value = voltval.List(y - 1)

       Next

Set xlSh = Nothing
Set xlApp = Nothing

End Sub
```

APPENDIX C

Table C.1 X-Ray, physical and chemical data of some phthalocyanine molecules (Oker, 1985)

	Free	Be	Mn	Fe	Co	Ni	Cu	Pt
Atomic number of metal	0	4	25	2 6	27	28	29	78
a, A	19.85	21.2	20.2	20.2	20.2	19.9	19.6	23.9
b, A	4.72	4.84	4.75	4.77	4.77	4.71	4.79	3.81
c, A	14.8	14.7	15.1	15.0	15.0	14.9	14.6	16.9
β	122.2^{o}	121.0^{o}	121.7^{o}	121.6^{o}	121.3^{o}	121.9^{o}	120.6^{o}	129.6^{o}
Space group	$P2_{1/a}$	$P2_{1/a}$	$P2_{1/a}$	$P2_{1/a}$	$P2_{1/a}$	$P2_{1/a}$	$P2_{1/a}$	$P2_{1/a}$
Mols. per cel	2	2	2	2	2	2	2	2
Molecular symmetry	Centro	Centro	Centro	Centro	Centro	Centro	Centro	Centro
Volume of Unit Cell, A	1173	1293	1233	1231	1235	1186	1180	1186
Density (Calc)	1.445	1.33	1.52	1.52	1.51	1.59	1.61	1.97
Molecular weight	514	521	567	568	571	571	576	707
Electrons per cell F(000)	532	536	578	580	582	584	586	784